On Thinning Ice:
Modeling Sea Ice as a Multiscale Composite Material

Kenneth M. Golden
Department of Mathematics, University of Utah

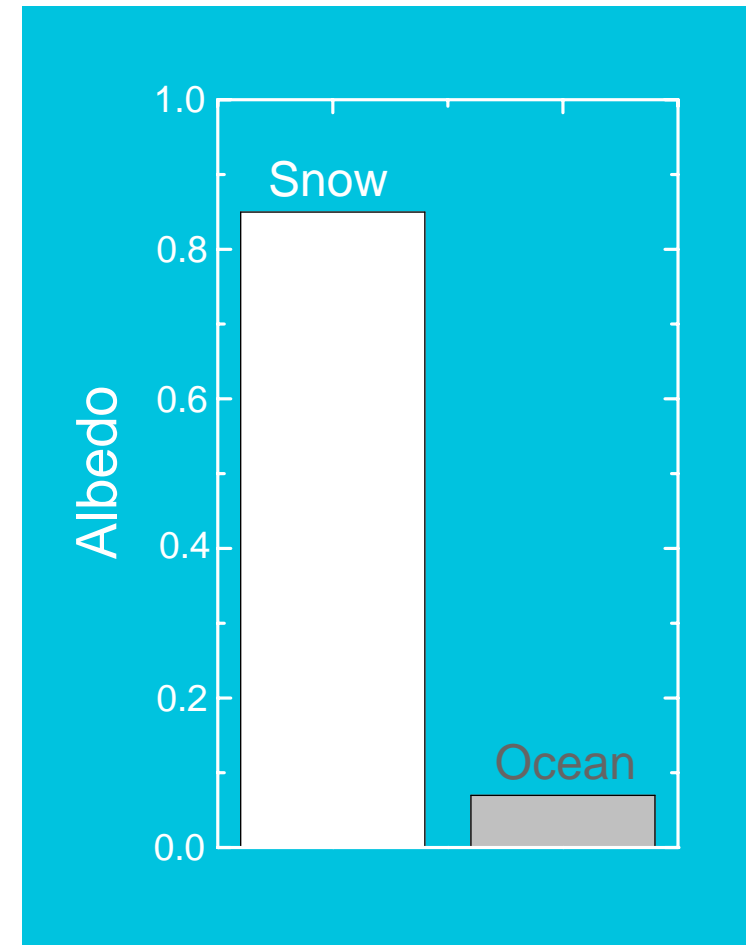**4th Annual Meeting of the
SIAM Texas-Louisiana Section
November 6, 2021**

Worby

polar ice caps critical to global climate in reflecting incoming solar radiation
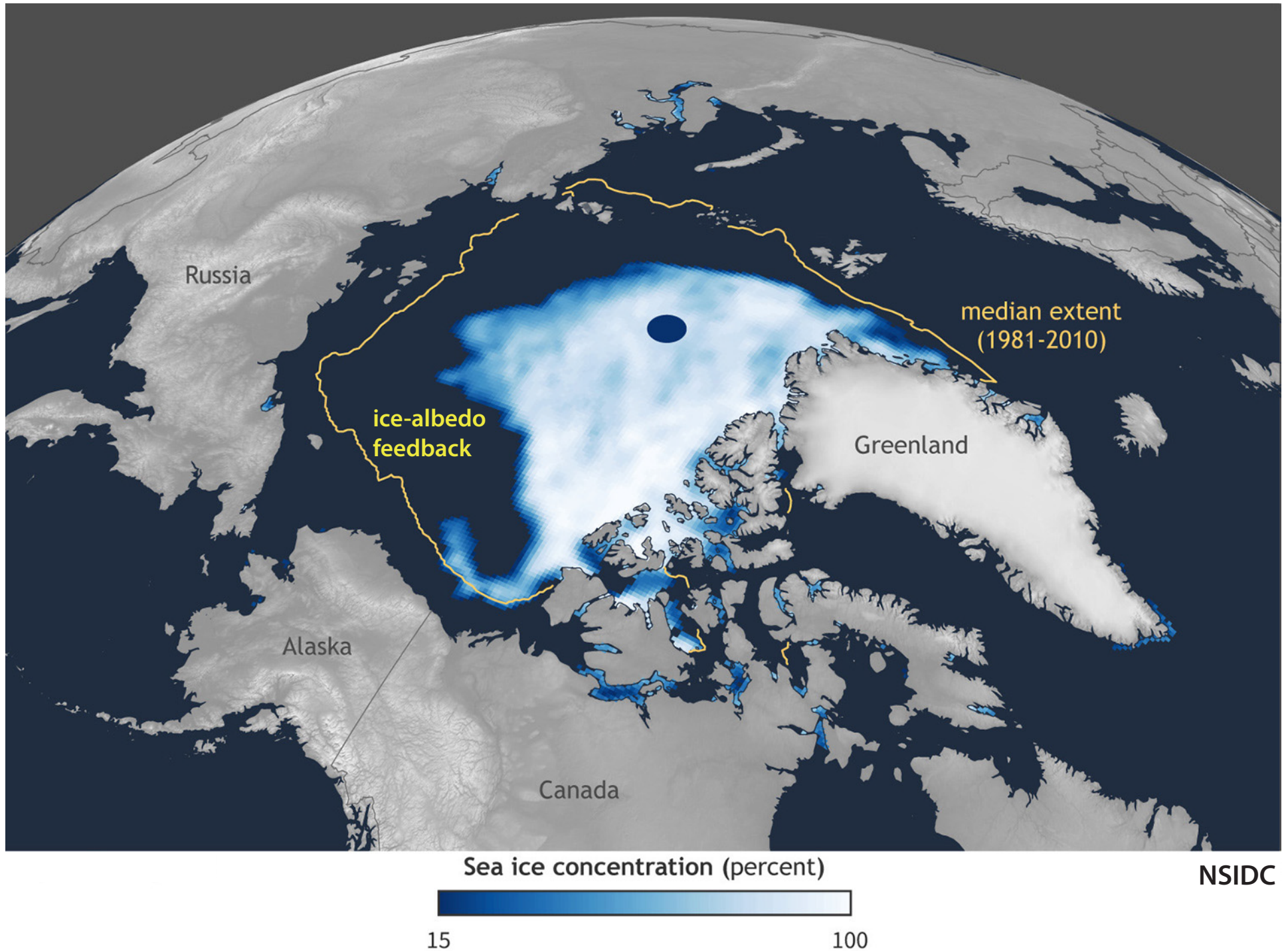
white snow and ice reflect

Earth's refrigerator
NASA

NASA

dark water and land absorb

$$albedo \quad \alpha = \frac{reflected\ sunlight}{incident\ sunlight}$$

Arctic sea ice extent   September 15, 2020

Russia

Greenland

median extent
(1981–2010)

ice-albedo
feedback

Alaska

Canada

Sea ice concentration (percent)

NSIDC

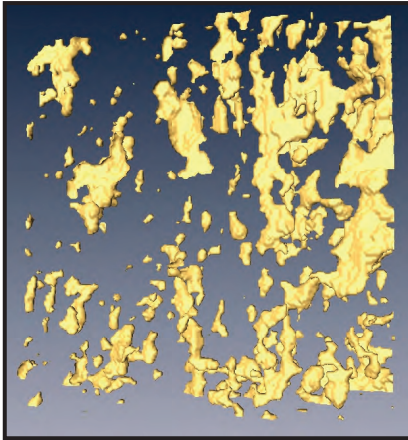15   100
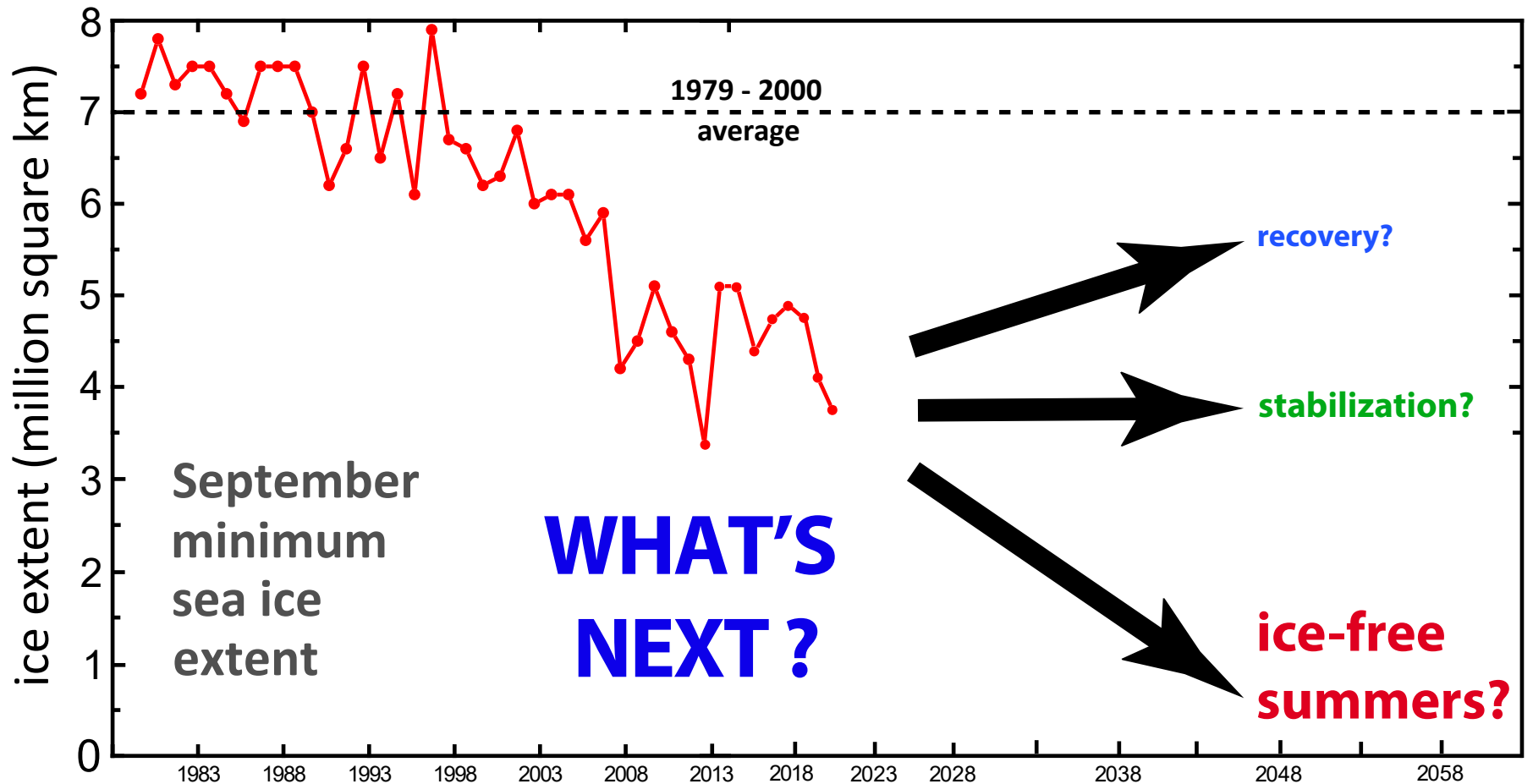
Sea Ice is a Multiscale Composite Material

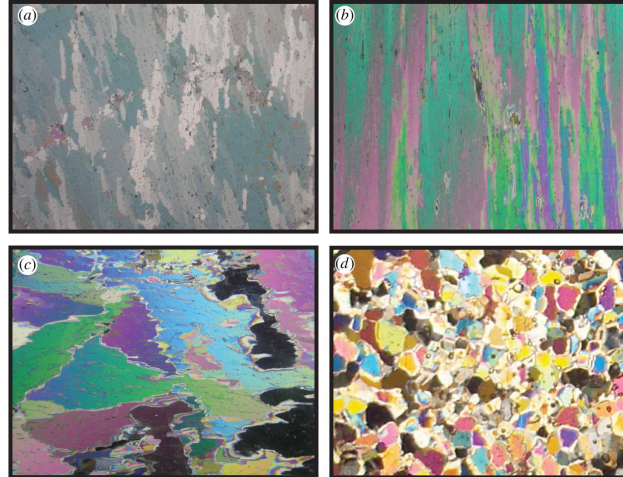## *microscale*

brine inclusions

Weeks & Assur 1969

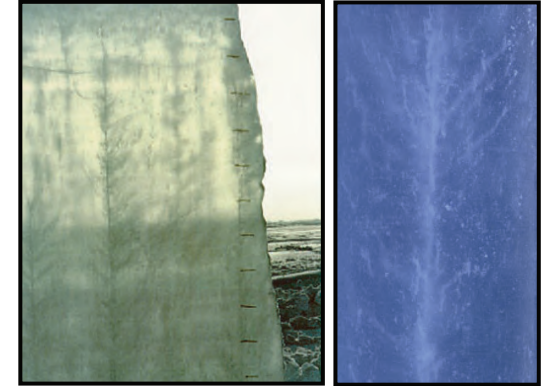H. Eicken
Golden *et al. GRL* 2007

polycrystals

Gully *et al. Proc. Roy. Soc. A* 2015

brine channels

D. Cole   K. Golden

millimeters   **centimeters**

mesoscale   *macroscale*
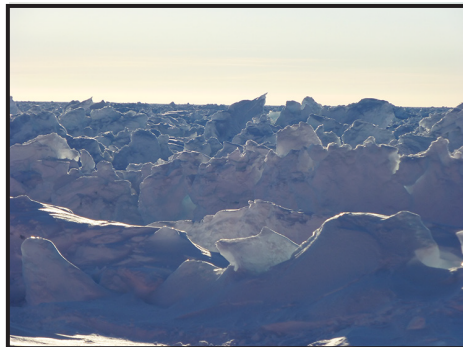
Arctic melt ponds

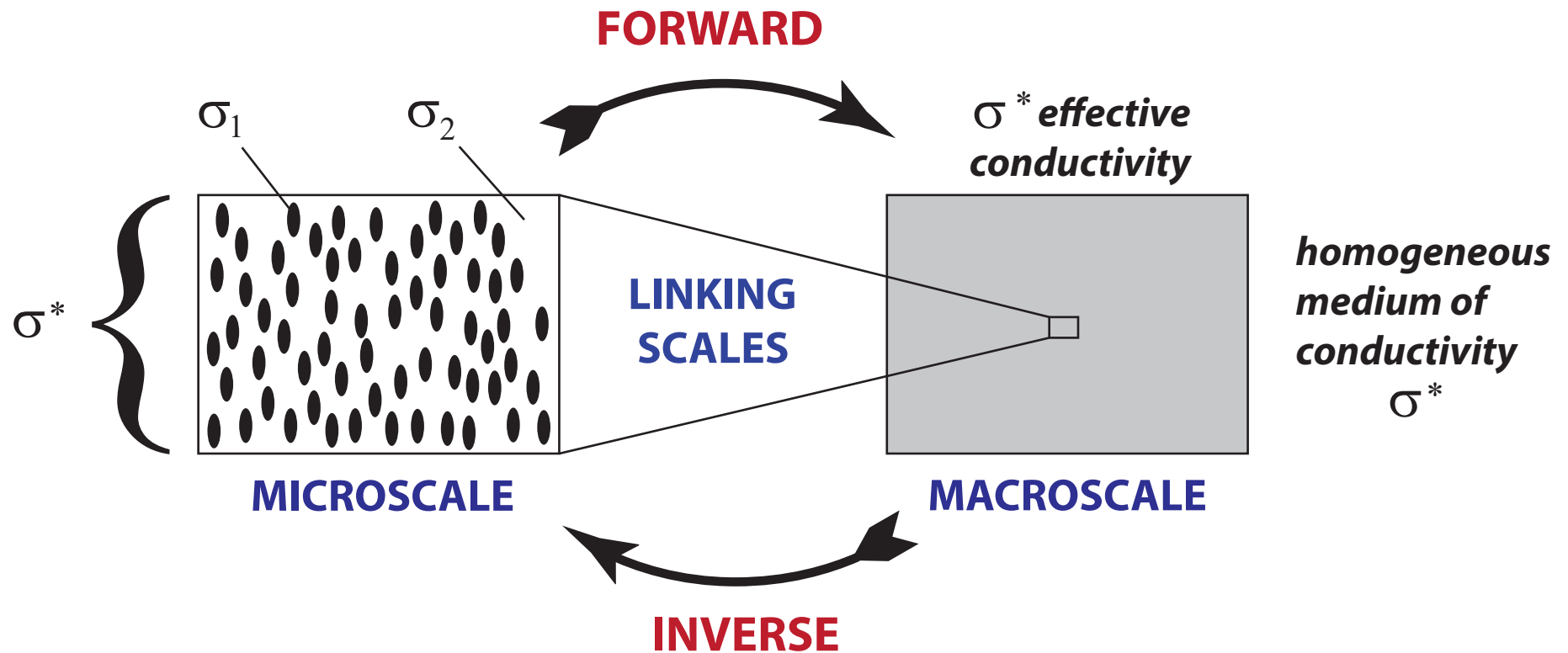K. Frey

Antarctic pressure ridges

K. Golden

sea ice floes

J. Weller

sea ice pack

NASA

meters   **kilometers**

HOMOGENIZATION for Composite Materials

FORWARD

σ_1 σ_2

σ^* effective conductivity

σ^*

LINKING SCALES

homogeneous medium of conductivity σ^*

MICROSCALE

MACROSCALE

INVERSE

Maxwell 1873 : effective conductivity of a dilute suspension of spheres
Einstein 1906 : effective viscosity of a dilute suspension of rigid spheres in a fluid

*Wiener 1912 : arithmetic and harmonic mean bounds on effective conductivity*
Hashin and Shtrikman 1962 : variational bounds on effective conductivity

widespread use of composites in late 20th century due in large part to advances in mathematically predicting their effective properties

What is this talk about?

Using methods of **homogenization and statistical physics** to model sea ice effective behavior and advance representation of sea ice in climate models, process studies, ...

MODELING SEA ICE

microscale

↓

mesoscale

↓
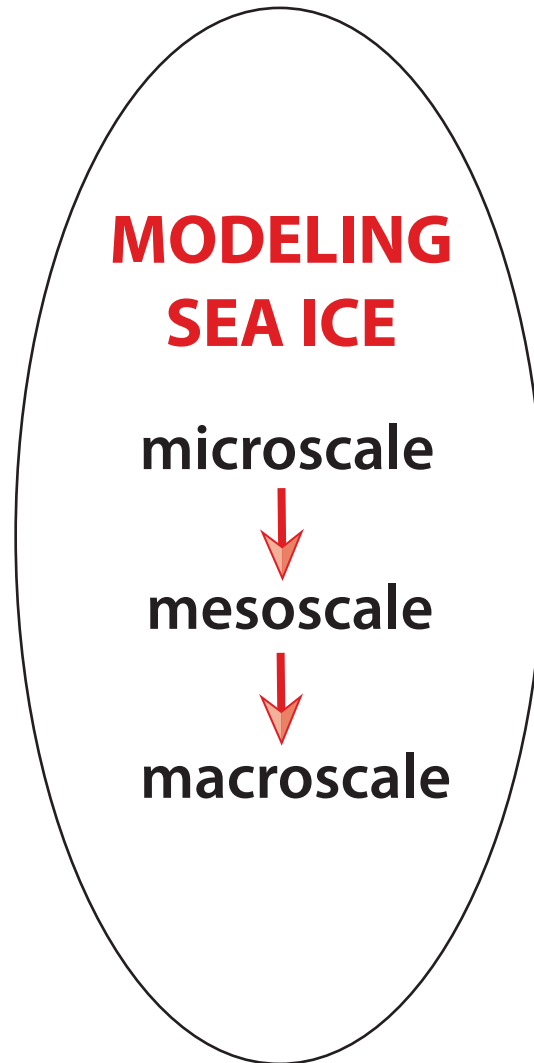
macroscale

A tour of key sea ice processes on micro, meso, and macro scales.

What is our research about?

Using methods of **homogenization and statistical physics** to model sea ice effective behavior and advance representation of sea ice in climate models, process studies, ...

Inputs, Ingredients

COMPOSITE MATERIALS

electrical engineering, stealth technology

porous media, oil extraction

statistical mechanics of ferromagnets

Anderson localization, semiconductor physics

random matrix theory

differential equations

Outputs, Impacts

CLIMATE MODELING

sea ice physics & biology

composites, polycrystals

remote sensing

advection diffusion

biomedical imaging, biomaterials, EPS

polar microbial ecology

MODELING SEA ICE

microscale

mesoscale

macroscale

How do scales interact in the sea ice system?

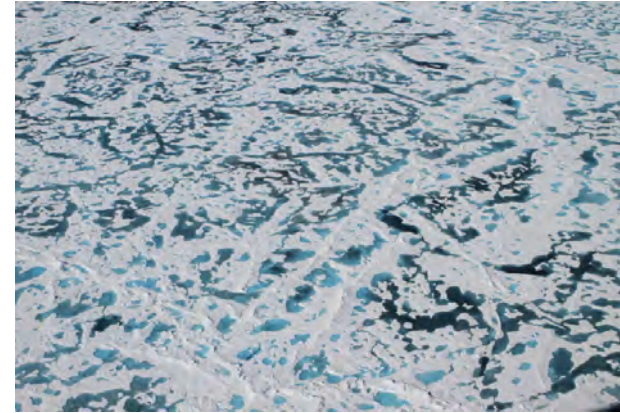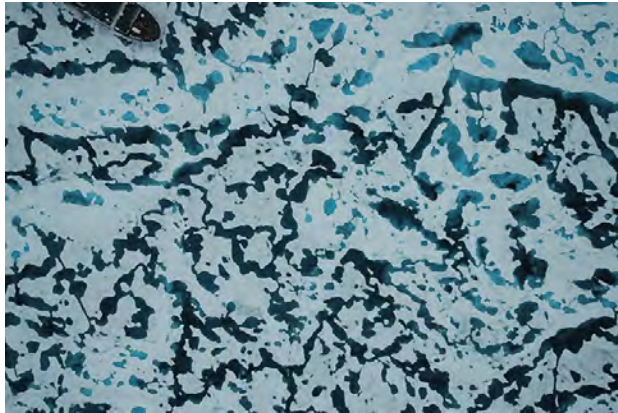
basin scale - grid scale albedo

NASA

Linking Scales

km scale melt ponds

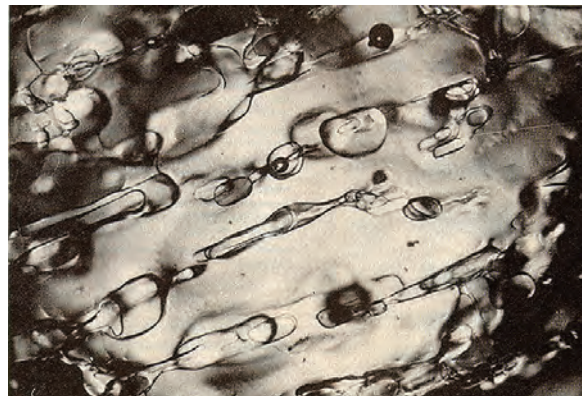Perovich

Linking Scales

mm scale brine inclusions

meter scale snow topography

microscale

fluid flow through the porous microstructure of sea ice governs key processes in polar climate and ecosystems

evolution of Arctic melt ponds and sea ice albedo

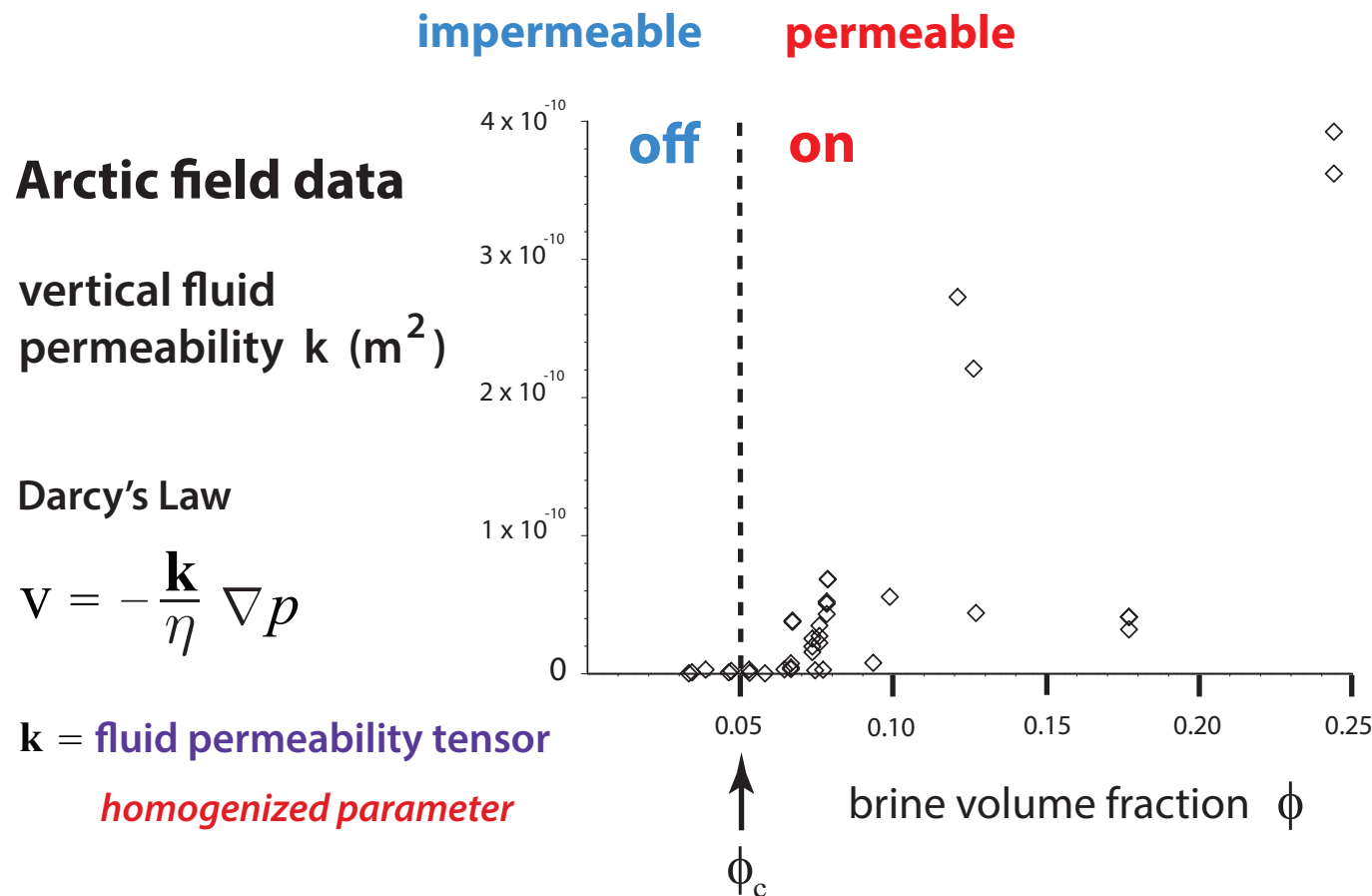K. Golden

nutrient flux for algal communities

C. Haas

ACE CRC

C. Krembs

22%

28%

26%

27%

September snow-ice estimates

0   25   50   75   100
percent snow ice

T. Maksym and T. Markus, 2008

Antarctic surface flooding and snow-ice formation

- evolution of salinity profiles
- ocean-ice-air exchanges of heat, CO_2

Critical behavior of fluid transport in sea ice

impermeable   **permeable**

Arctic field data

vertical fluid
permeability k (m^2)

Darcy's Law

$$\mathbf{v} = -\frac{\mathbf{k}}{\eta} \nabla p$$

$\mathbf{k}$ = **fluid permeability tensor**

homogenized parameter

off   *on*

brine volume fraction ϕ

ϕ_c

"on - off" switch for fluid flow

critical brine volume fraction $\phi_c \approx 5\% \longleftrightarrow T_c \approx -5°C, \ S \approx 5$ ppt

RULE OF FIVES

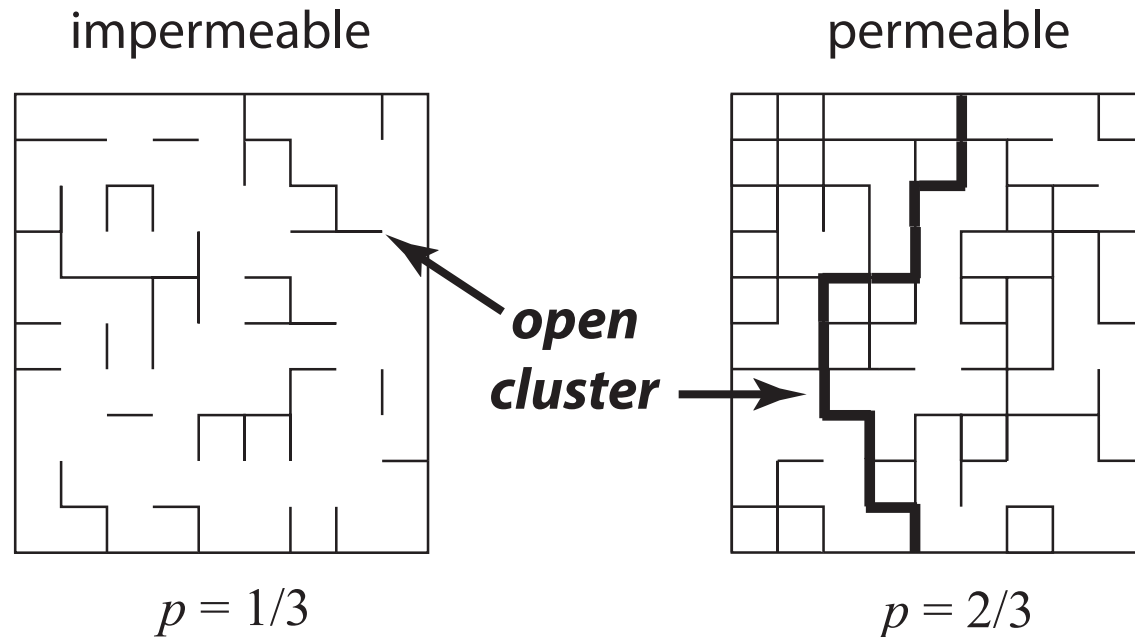**Golden, Ackley, Lytle   Science   1998**
Golden, Eicken, Heaton, Miner, Pringle, Zhu   GRL 2007
Pringle, Miner, Eicken, Golden   J. Geophys. Res.   2009

percolation theory

probabilistic theory of connectedness

percolation theory — impermeable ($p = 1/3$) and permeable ($p = 2/3$) lattices with **open cluster** labeled.

$$\text{bond} \longrightarrow \begin{array}{ll} \textbf{\textit{open}} & \textit{with probability } p \\ \textbf{\textit{closed}} & \textit{with probability } 1\text{-}p \end{array}$$
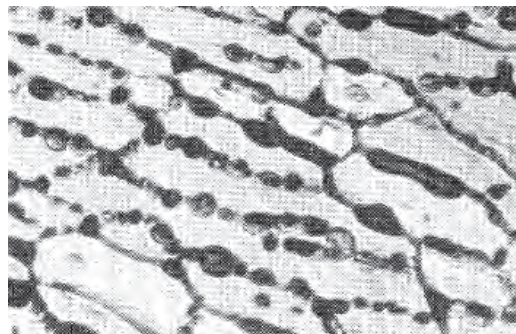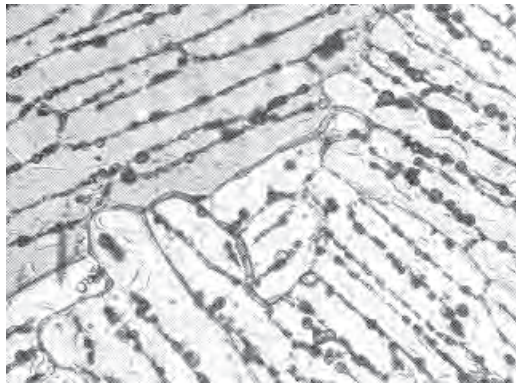
percolation threshold

$$p_c = 1/2 \quad \text{for} \quad d = 2$$

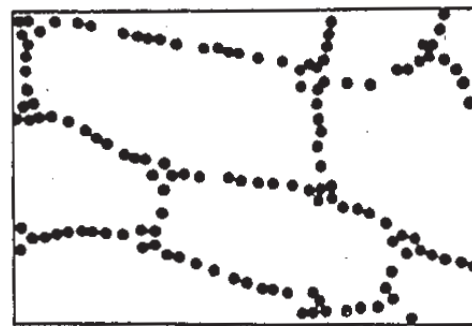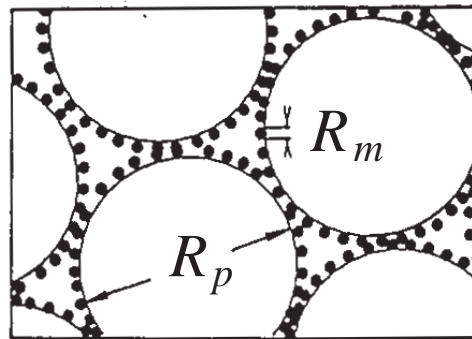**smallest p for which there is an infinite open cluster**

Continuum percolation model for ***stealthy*** materials applied to sea ice microstructure explains **Rule of Fives** and Antarctic data on ice production and algal growth
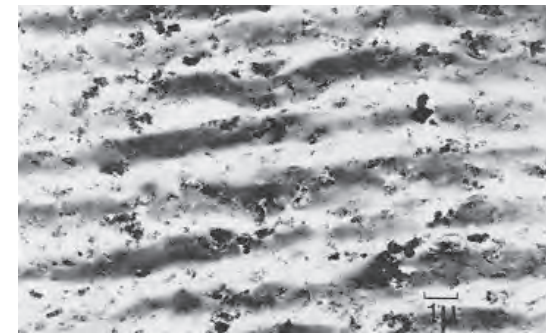
$\phi_c \approx 5 \%$ Golden, Ackley, Lytle, *Science,* 1998

sea ice

R_m

R_p

compressed powder
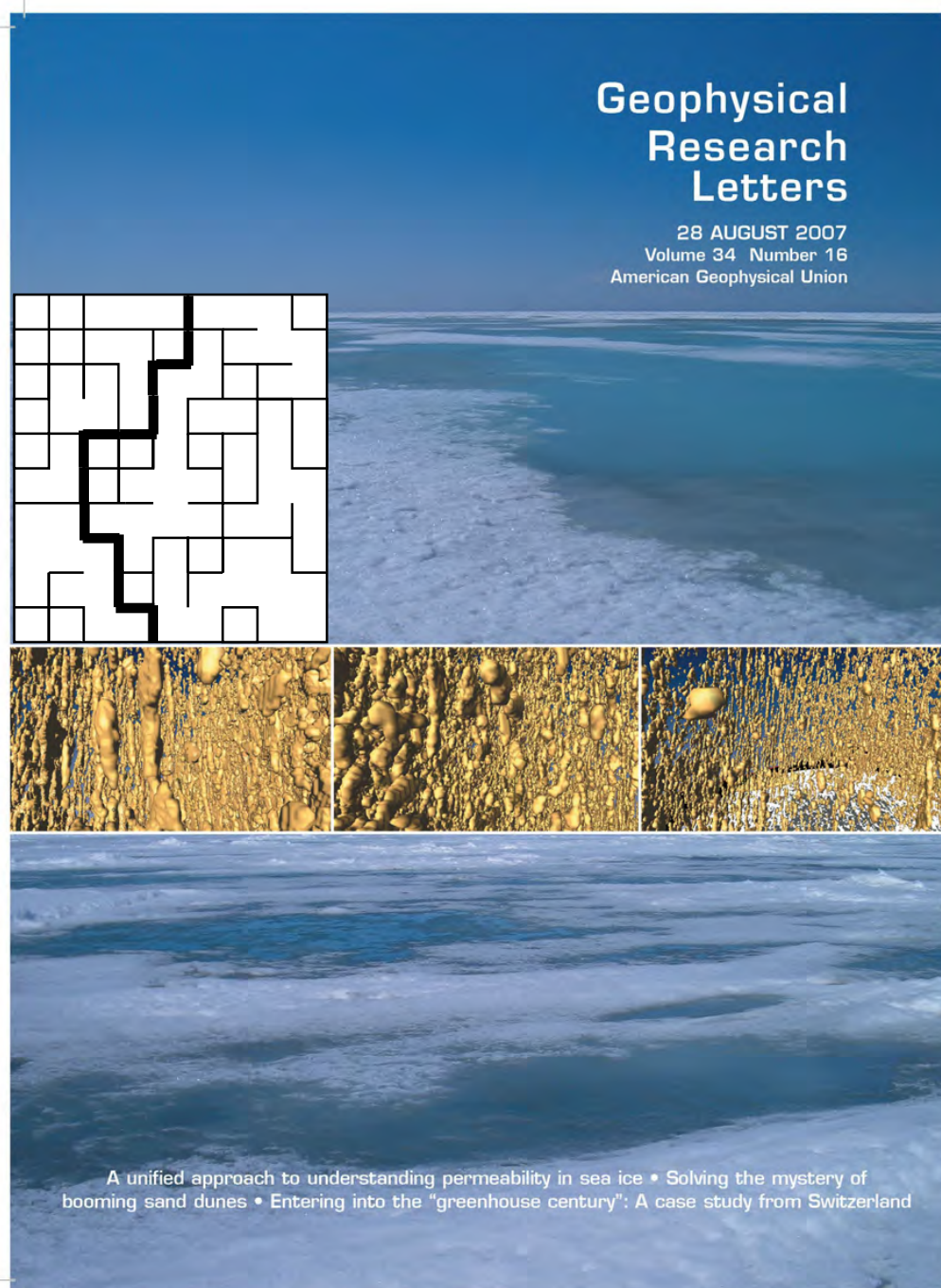

B-2 Stealth Bomber
F-117 Nighthawk
Stealthy Helicopters

radar absorbing composite

sea ice is radar absorbing

Thermal evolution of permeability and microstructure in sea ice

Golden, Eicken, Heaton, Miner, Pringle, Zhu,   Geophysical Research Letters   2007

**percolation theory
for fluid permeability**

$$k(\phi) = k_0 (\phi - 0.05)^2$$

critical
exponent

t

$$k_0 = 3 \times 10^{-8} \ \mathrm{m}^2$$

**critical path analysis
Kozlov and Golden, 1990s**

**hierarchical + network models
rigorous bounds**

**X-ray tomography for
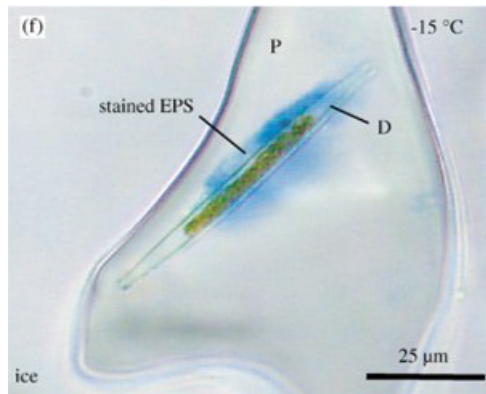brine inclusions**

confirms rule of fives

**Pringle, Miner, Eicken, Golden
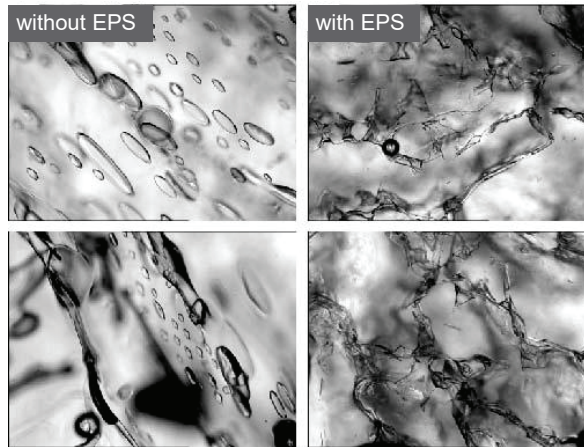J. Geophys. Res. 2009**

**theories agree closely
with field data**

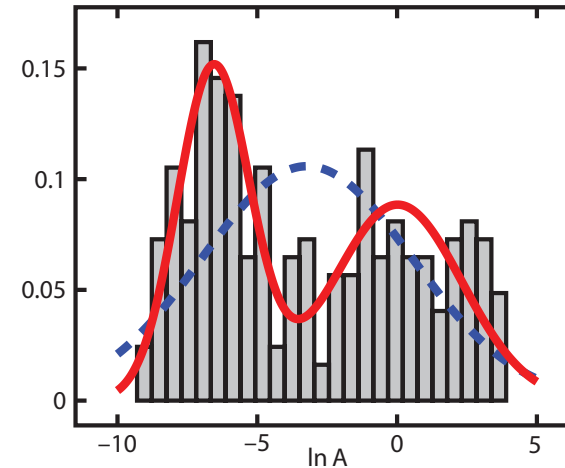# Sea ice algae secrete extracellular polymeric substances (EPS) affecting evolution of brine microstructure.

How does EPS affect fluid transport? How does the biology affect the physics?

Krembs

Krembs, Eicken, Deming, PNAS 2011

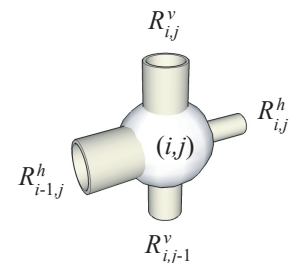***RANDOM
PIPE
MODEL***
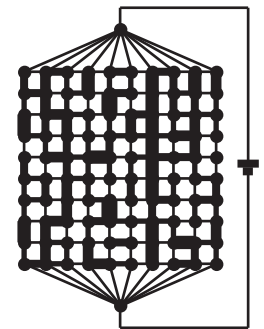
- 2D random pipe model with bimodal distribution of pipe radii

- Rigorous bound on permeability *k;* results predict observed drop in *k*

Steffen, Epshteyn, Zhu, Bowler, Deming, Golden
Multiscale Modeling and Simulation, 2018

$R_{i,j}^{v}$
$R_{i,j}^{h}$
(i,j)
$R_{i-1,j}^{h}$
$R_{i,j-1}^{v}$

Zhu, Jabini, Golden, Eicken, Morris
***Ann. Glac.* 2006**

Notices

of the American Mathematical Society

Climate Change and
the Mathematics of
Transport in Sea Ice

page 562

Mathematics and the
Internet: A Source of
Enormous Confusion
and Great Potential

page 586

photo by Jan Lieser

Real analysis in polar coordinates (see page 613)
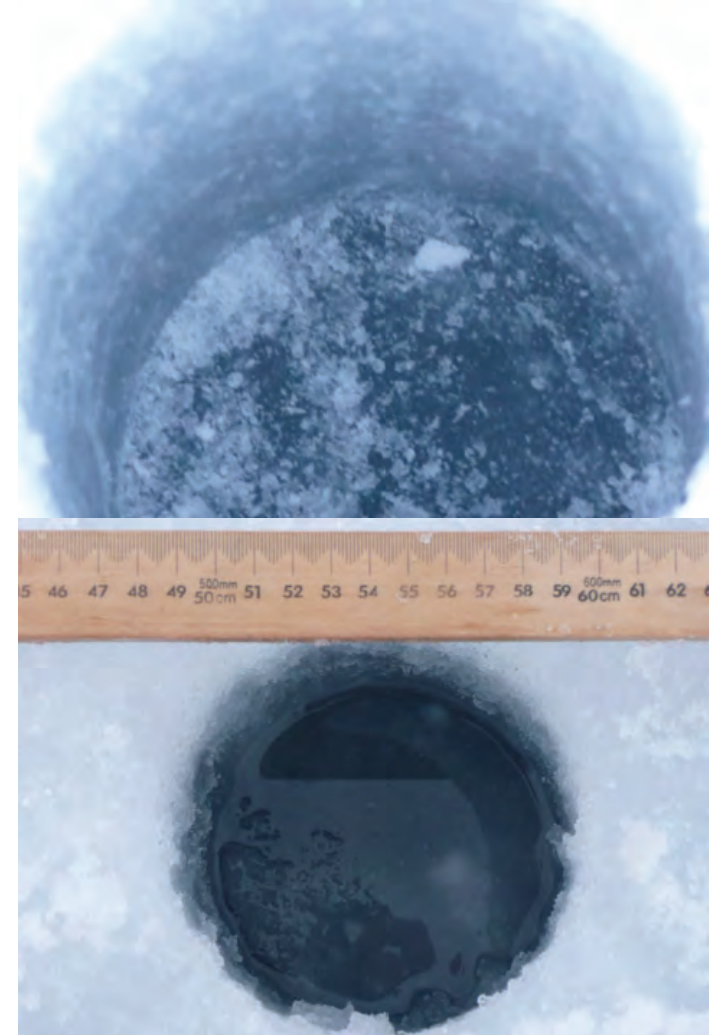
*measuring
fluid permeability
of Antarctic sea ice*

SIPEX 2007

Remote sensing of sea ice

INVERSE PROBLEM

Recover sea ice properties from electromagnetic (EM) data

$$\varepsilon^*$$

effective complex permittivity (dielectric constant, conductivity)

sea ice thickness
ice concentration

brine volume fraction
brine inclusion connectivity

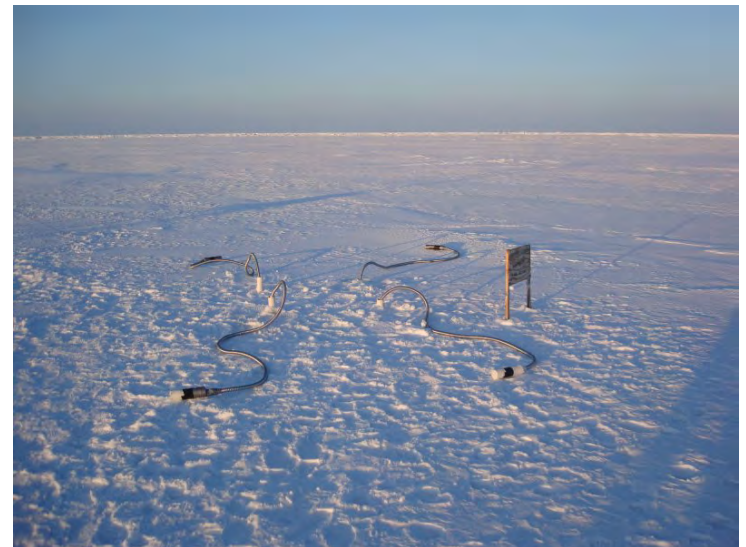# Effective complex permittivity of a two phase composite in the quasistatic (long wavelength) limit

ϵ_1 ϵ_2

$$\left. \begin{array}{c} \end{array} \right\} \epsilon^*$$
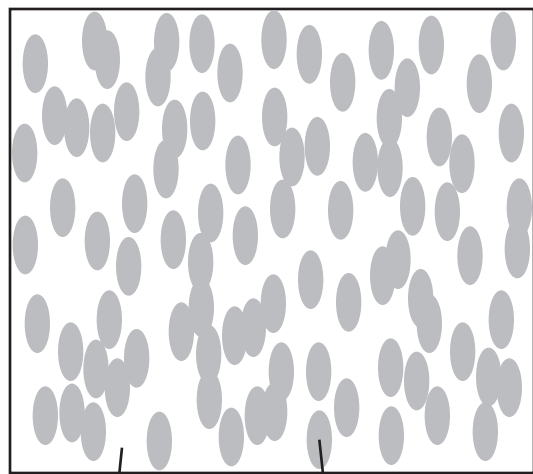
$$D = \epsilon E$$

$$\nabla \cdot D = 0$$

$$\nabla \times E = 0$$

$$\langle D \rangle = \epsilon^* \langle E \rangle$$

$p_1 \, , \, p_2$ = volume fractions of the components

$$\epsilon^* = \epsilon^* \left(\frac{\epsilon_1}{\epsilon_2} \, , \, \text{composite geometry} \right)$$

What are the effective propagation characteristics of an EM wave (radar, microwaves) in the medium?

Analytic Continuation Method for Homogenization

Bergman (1978), Milton (1979), Golden and Papanicolaou (1983), Theory of Composites, Milton (2002)

Stieltjes integral representation for homogenized parameter

separates geometry from parameters

geometry

$$F(s) = 1 - \frac{\epsilon^*}{\epsilon_2} = \int_0^1 \frac{d\mu(z)}{s - z}$$

$$s = \frac{1}{1 - \epsilon_1 / \epsilon_2}$$

material parameters

μ

- spectral measure of self adjoint operator $\Gamma\chi$
- mass = p_1
- higher moments depend on n-point correlations

$$\Gamma = \nabla(-\Delta)^{-1}\nabla \cdot$$

$\chi =$ characteristic function of the brine phase

$$E = s \, (s + \Gamma\chi)^{-1} e_k$$

$$\Gamma\chi : \textbf{microscale} \longrightarrow \textbf{macroscale}$$

$$\Gamma\chi \textit{ links scales}$$

Golden and Papanicolaou, Comm. Math. Phys. 1983
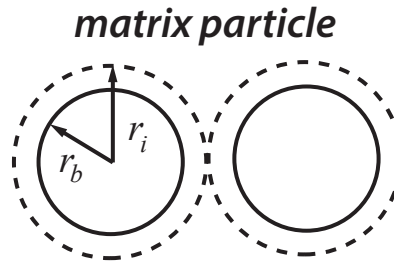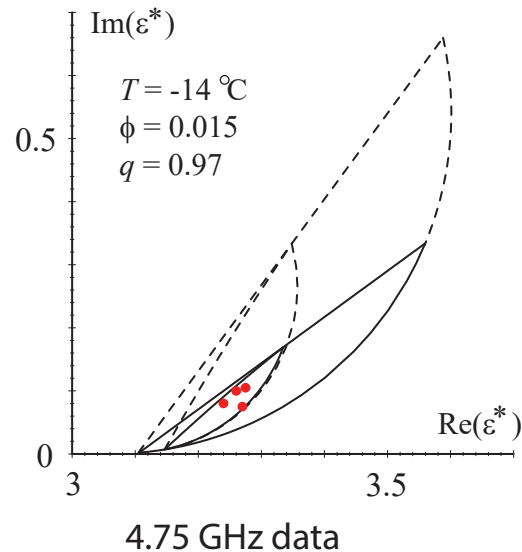
This representation distills the complexities of mixture geometry into the spectral properties of an operator like the Hamiltonian in physics.

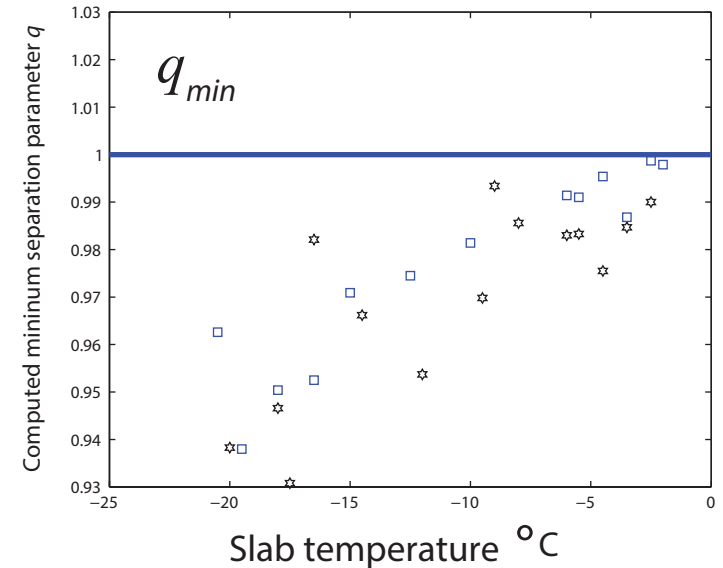# forward and inverse bounds on the complex permittivity of sea ice

forward bounds

$$\text{Im}(\varepsilon^*)$$

$T = -14\ ^\circ\text{C}$
$\phi = 0.015$
$q = 0.97$

0.5

$\text{Re}(\varepsilon^*)$

0

3 3.5

4.75 GHz data

matrix particle

r_i

r_b

$$q = r_b / r_i$$

$$0 < q < 1$$

Golden 1995, 1997

inverse bounds

Computed minimum separation parameter q

q_{min}

Slab temperature $^\circ$C

Inverse Homogenization

Cherkaev and Golden (1998), Day and Thorpe (1999),
Cherkaev (2001), McPhedran, McKenzie, Milton (1982),
Theory of Composites, Milton (2002)

$$\varepsilon^* \longrightarrow$$ **composite geometry (spectral measure μ)**

inverse bounds and recovery of brine porosity

Gully, Backstrom, Eicken, Golden
Physica B, 2007

inversion for brine inclusion separations in sea ice from measurements of effective complex permittivity ε^*

rigorous inverse bound on spectral gap

construct algebraic curves which bound admissible region in (p,q)-space

Orum, Cherkaev, Golden
Proc. Roy. Soc. A, 2012

direct calculation of spectral measures

- depends only on the composite geometry

- discretization of microstructural image gives binary network

- fundamental operator becomes a random matrix

- spectral measure computed from eigenvalues and eigenvectors

once we have the spectral measure μ it can be used in Stieltjes integrals for other transport coefficients:

electrical and thermal conductivity, complex permittivity, magnetic permeability, diffusion, fluid flow properties
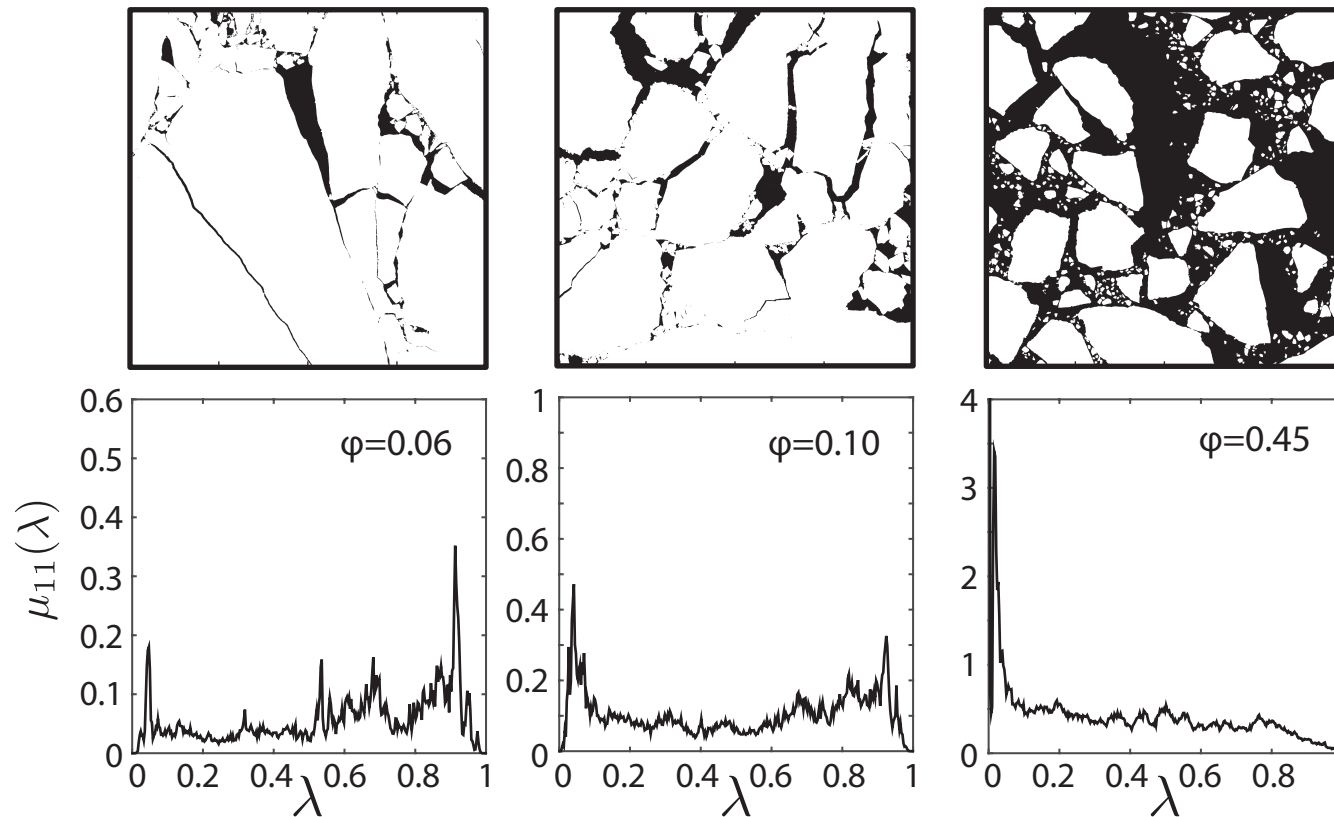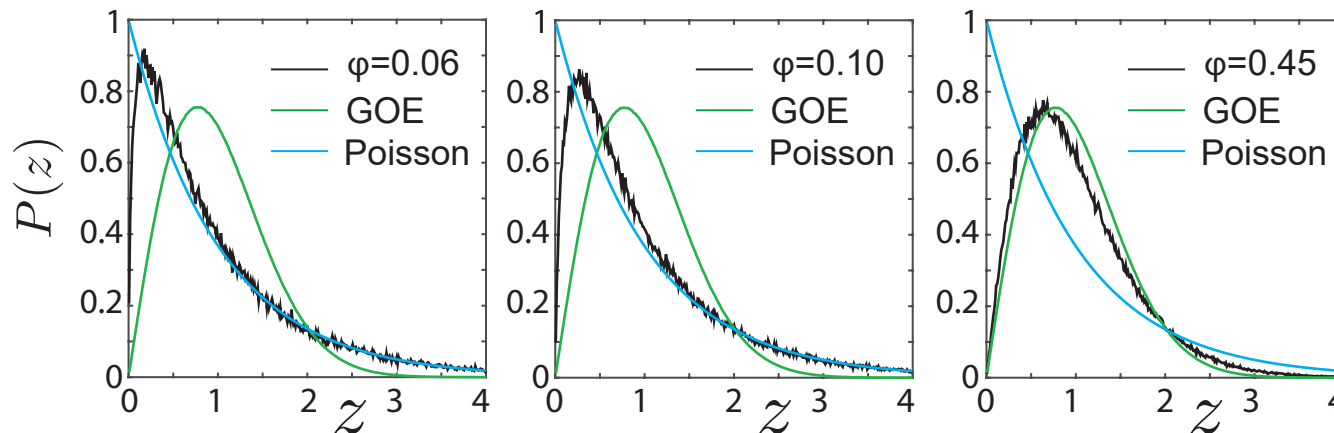
earlier studies of spectral measures

Day and Thorpe 1996
Helsing, McPhedran, Milton 2011

Spectral computations for sea ice floe configurations

extended

$\psi_\alpha(x)$
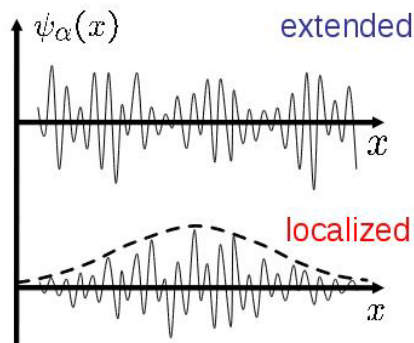
localized

electronic transport in semiconductors

metal / insulator transition

localization

Anderson 1958
Mott 1949
Shklovshii et al 1993
Evangelou 1992

Anderson transition in wave physics:
quantum, optics, acoustics, water waves, ...

from analysis of spectral measures for brine, melt ponds, ice floes

we find percolation-driven

Anderson transition for classical transport in composites
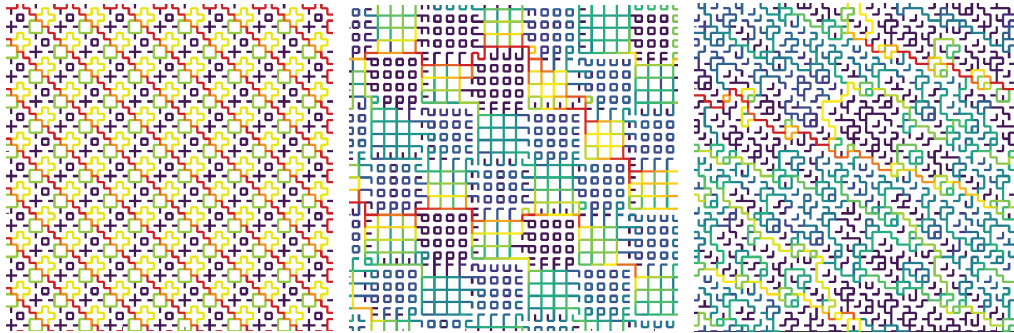*Murphy, Cherkaev, Golden   Phys. Rev. Lett.   2017*

PERCOLATION
TRANSITION ➔ universal eigenvalue statistics (GOE)
extended states, mobility edges

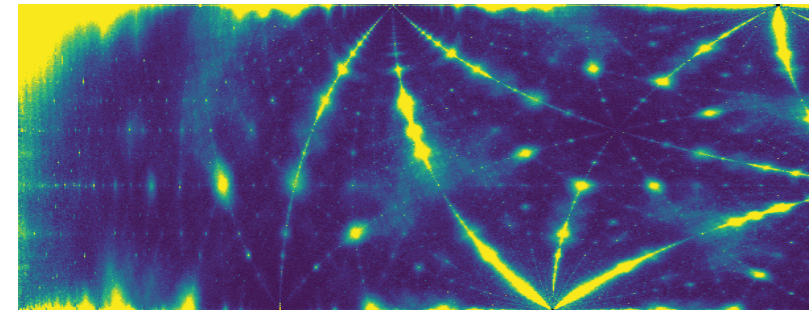**-- but with NO wave interference or scattering effects ! --**

Order to disorder in quasiperiodic composites

Morison, Murphy, Cherkaev, Golden 2021

Parameterized Moiré Pattern Creates Tunable Microgeometry

Poisson

Wigner-Dyson

Anderson transition as QP is tuned

parameter space

periodic ⟶ quasiperiodic

electric field strength

$\varphi = 0$ $\varphi = 1/8$ $\varphi = 1/2$ $\varphi = 2$ random

RRN at percolation threshold

spectral measure

μ

10^{-4}
10^{-6}
10^{-8}
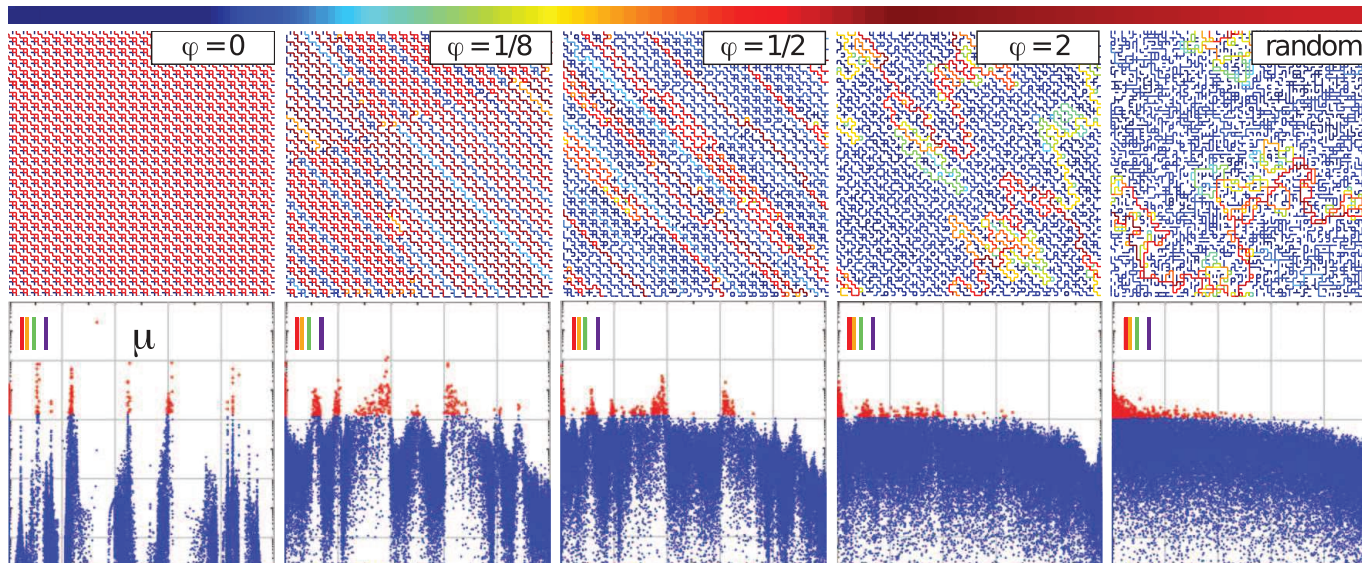
we bring the framework of solid state physics of electronic transport and band gaps in semiconductors to classical transport in periodic and quasiperiodic composites

photonic crystals and quasicrystals

Bounds on the complex permittivity of polycrystalline materials by analytic continuation

Adam Gully, Joyce Lin, Elena Cherkaev, Ken Golden

- **Stieltjes integral representation for effective complex permittivity**

  Milton (1981, 2002), Barabash and Stroud (1999), ...

- **Forward and inverse bounds**

  orientation statistics

- **Applied to sea ice using two-scale homogenization**

- **Inverse bounds give method for distinguishing ice types using remote sensing techniques**
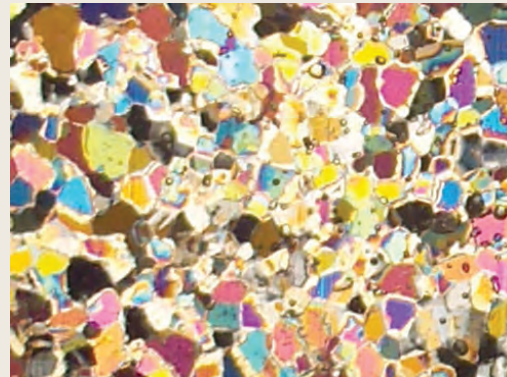
PROCEEDINGS A

350 YEARS
OF SCIENTIFIC
PUBLISHING

An invited review commemorating 350 years of scientific publishing at the Royal Society

A method to distinguish between different types of sea ice using remote sensing techniques

A computer model to determine how a human should walk so as to expend the least energy

THE
ROYAL
SOCIETY
PUBLISHING

21/01/15 1:47 PM

higher threshold for fluid flow in granular sea ice
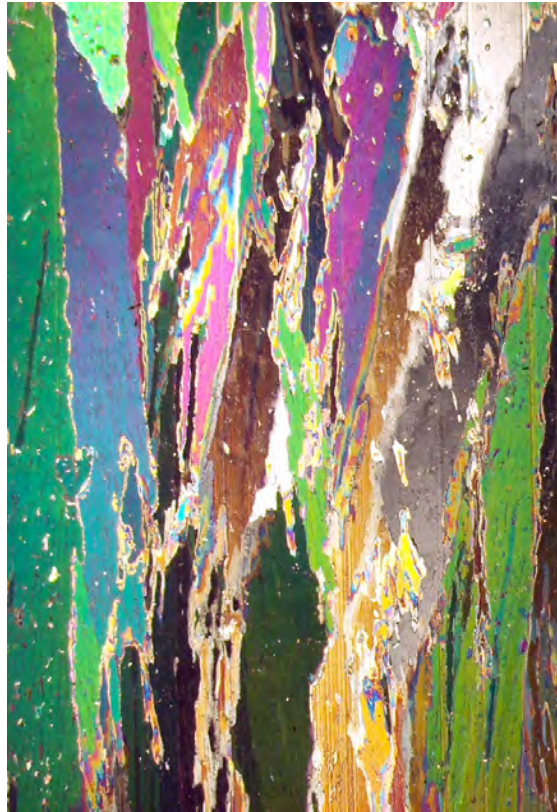
microscale details impact "mesoscale" processes

nutrient fluxes for microbes
melt pond drainage
snow-ice formation

columnar   granular

5%   10%

Golden, Sampson, Gully, Lubbers, Tison 2021

electromagnetically distinguishing ice types
Kitsel Lusted, Elena Cherkaev, Ken Golden

mesoscale

wave propagation in the marginal ice zone (MIZ)

Stieltjes integral representation and bounds for the complex viscoelasticity of the ice - ocean layer

Sampson, Murphy, Cherkaev, Golden 2021

first theory of key parameter in wave-ice interactions only fitted to wave data before
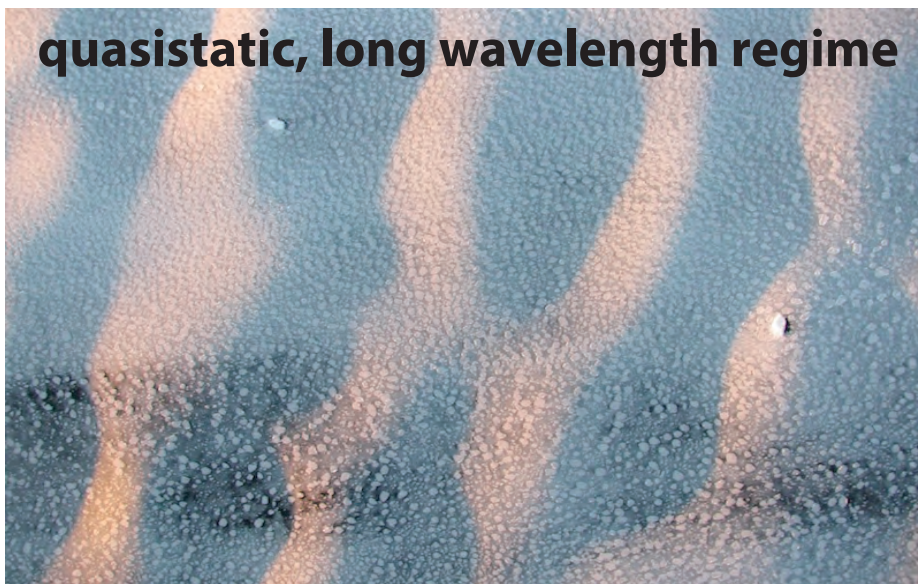
Analytic Continuation Method
Bergman (78) - Milton (79)
integral representation for ε^*
Golden and Papanicolaou (83)

Milton, *Theory of Composites* (02)

quasistatic, long wavelength regime

homogenized parameter depends on sea ice concentration and ice floe geometry

like EM waves

advection enhanced diffusion

effective diffusivity

nutrient and salt transport in sea ice
heat transport in sea ice with convection
sea ice floes in winds and ocean currents
tracers, buoys diffusing in ocean eddies
diffusion of pollutants in atmosphere

advection diffusion equation with a velocity field $\vec{u}$

$$\frac{\partial T}{\partial t} + \vec{u} \cdot \vec{\nabla} T = \kappa_0 \Delta T$$

$$\vec{\nabla} \cdot \vec{u} = 0$$

homogenize

$$\frac{\partial \overline{T}}{\partial t} = \kappa^* \Delta \overline{T}$$
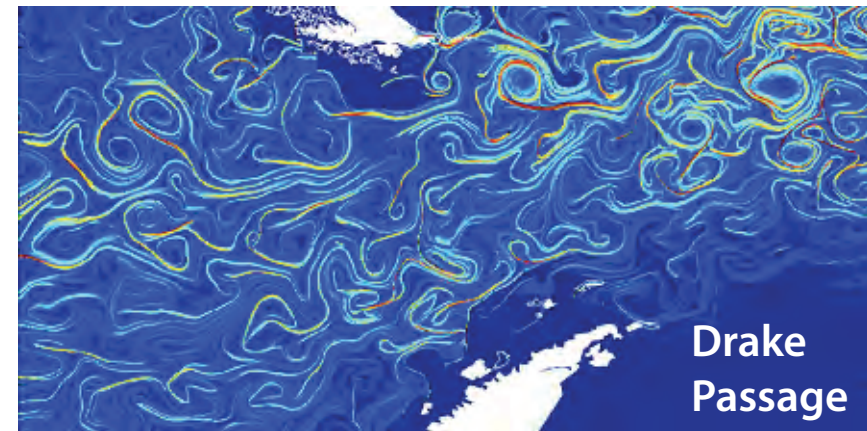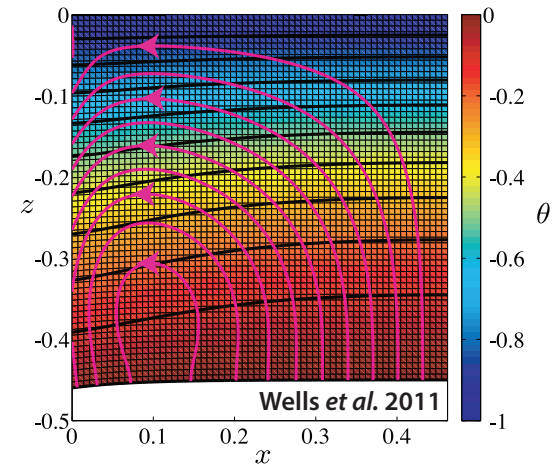
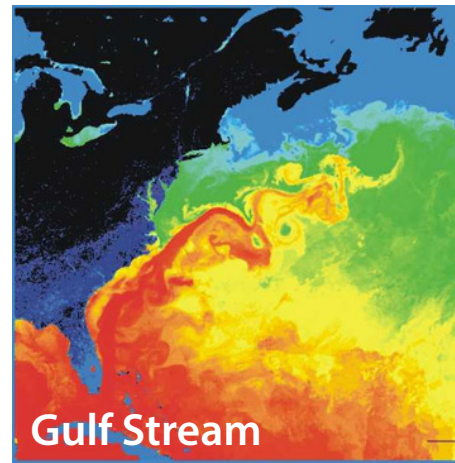κ^* **effective diffusivity**

Stieltjes integral for κ^* with spectral measure

Avellaneda and Majda, PRL 89, CMP 91

Murphy, Cherkaev, Xin, Zhu, Golden, *Ann. Math. Sci. Appl.* 2017
Murphy, Cherkaev, Zhu, Xin, Golden, *J. Math. Phys.* 2020

Gulf Stream

Wells *et al.* 2011

Drake Passage

sea ice vortices

Masters, 1989

tracers flowing through inverted sea ice blocks

Stieltjes Integral Representation for Advection Diffusion

$$\kappa^* = \kappa \left(1 + \int_{-\infty}^{\infty} \frac{d\mu(\tau)}{\kappa^2 + \tau^2} \right), \quad F(\kappa) = \int_{-\infty}^{\infty} \frac{d\mu(\tau)}{\kappa^2 + \tau^2}$$

- μ is a positive definite measure corresponding to the spectral resolution of the self-adjoint operator $i\Gamma H\Gamma$

- $H =$ stream matrix , $\kappa =$ local diffusivity

- $\Gamma := -\nabla(-\Delta)^{-1}\nabla\cdot$, Δ is the Laplace operator

- $i\Gamma H\Gamma$ is bounded for time independent flows

- $F(\kappa)$ is analytic off the spectral interval in the κ-plane

rigorous framework for numerical computations of spectral measures and effective diffusivity for model flows

new integral representations, theory of moment calculations

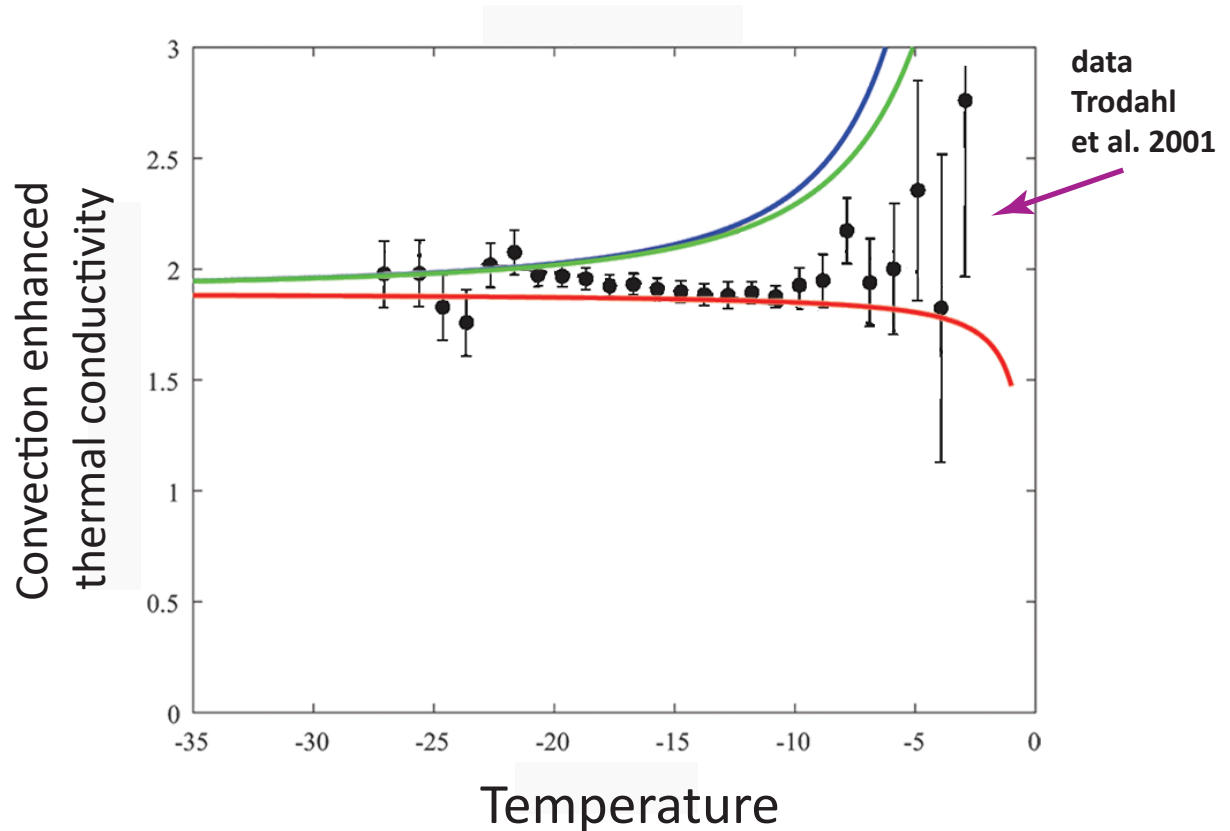**separation of material properties and flow field**

Rigorous bounds on convection enhanced thermal conductivity of sea ice

Kraitzman, Hardenbrook, Dinh, Murphy, Zhu, Cherkaev, Golden 2021
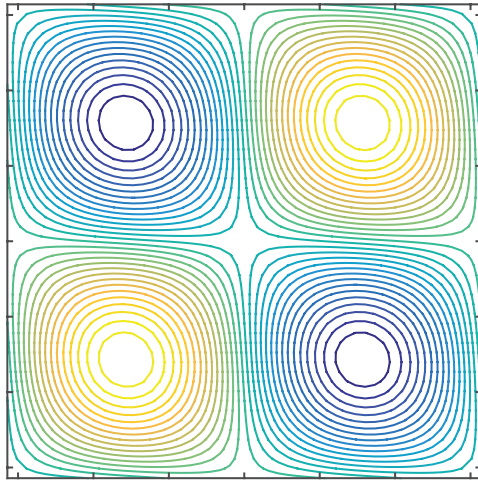
cat's eye flow model for
brine convection cells

similar bounds
for shear flows

data
Trodahl
et al. 2001

rigorous Padé bounds from Stieltjes integral +
analytical calculations of moments of measure

rigorous bounds assuming information on flow field INSIDE inclusions

Kraitzman, Cherkaev, Golden
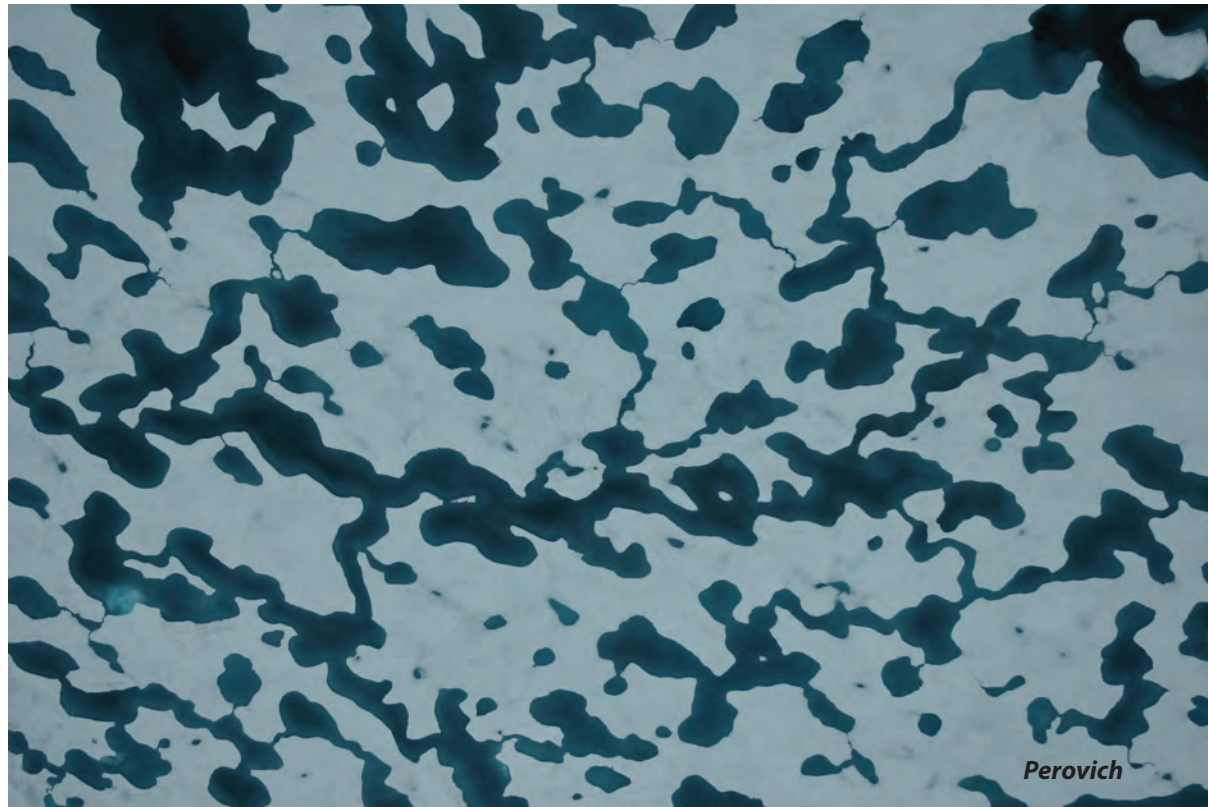*SIAM J. Appl. Math.* (in revision), 2021

melt pond formation and albedo evolution:

- **major drivers in polar climate**
- **key challenge for global climate models**

numerical models of melt pond evolution, including topography, drainage (permeability), etc.

Lüthje, Feltham, Taylor, Worster 2006

Skyllingstad, Paulson, Perovich 2009

Flocco, Feltham 2007

Flocco, Feltham, Hunke 2012

Perovich

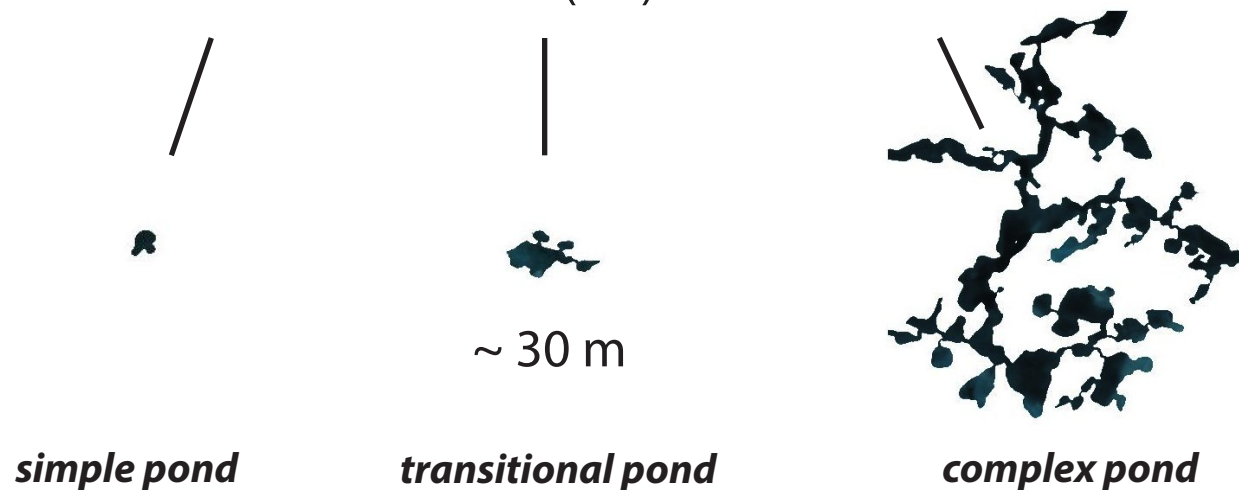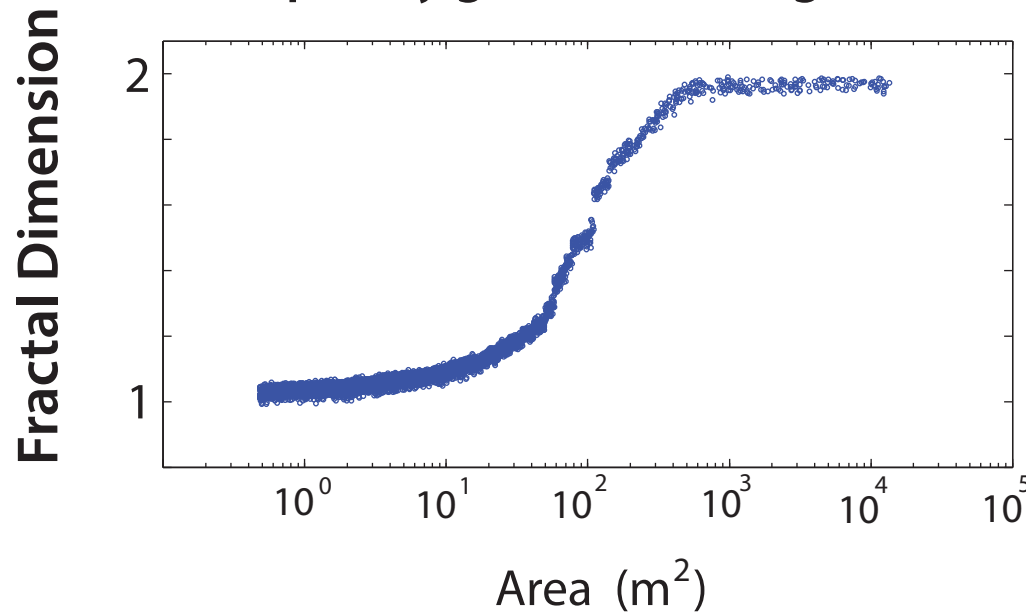## Are there universal features of the evolution similar to phase transitions in statistical physics?

Transition in the fractal geometry of Arctic melt ponds

Christel Hohenegger, Bacim Alali, Kyle Steffen, Don Perovich, Ken Golden

The Cryosphere, 2012

complexity grows with length scale

~ 30 m

simple pond   transitional pond   complex pond

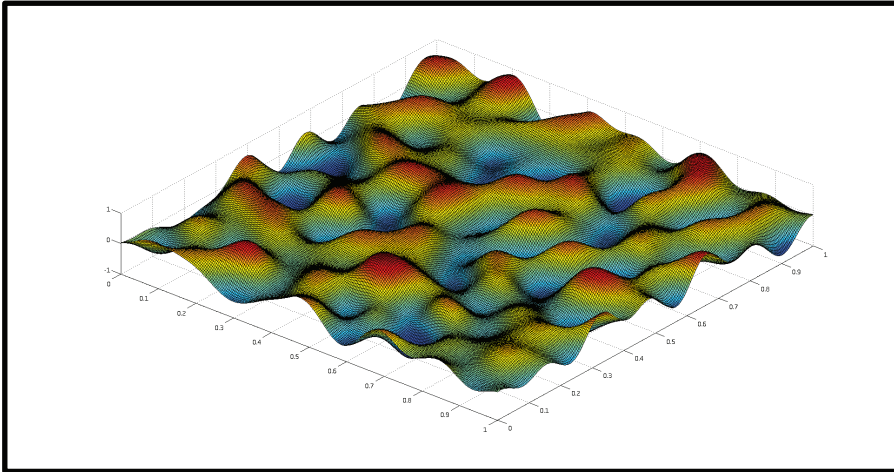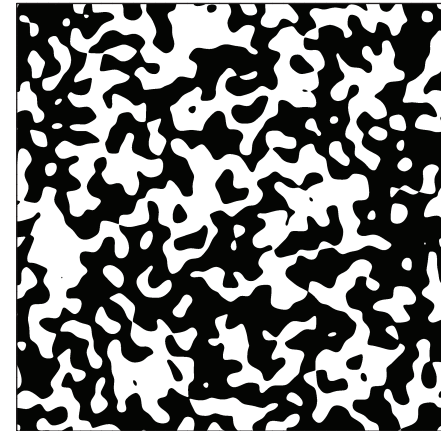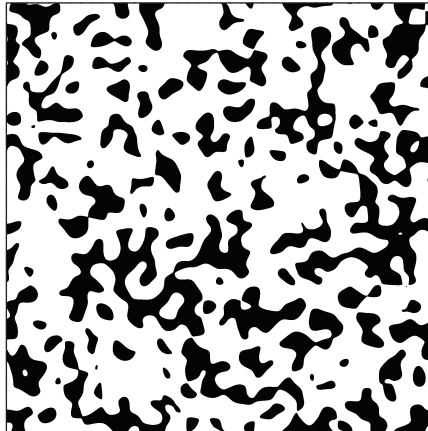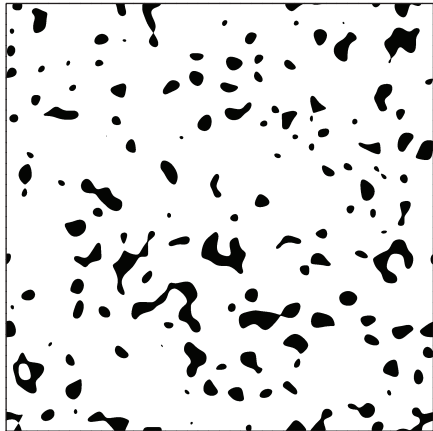# Continuum percolation model for melt pond evolution
level sets of random surfaces

Brady Bowen, Court Strong, Ken Golden, J. Fractal Geometry 2018
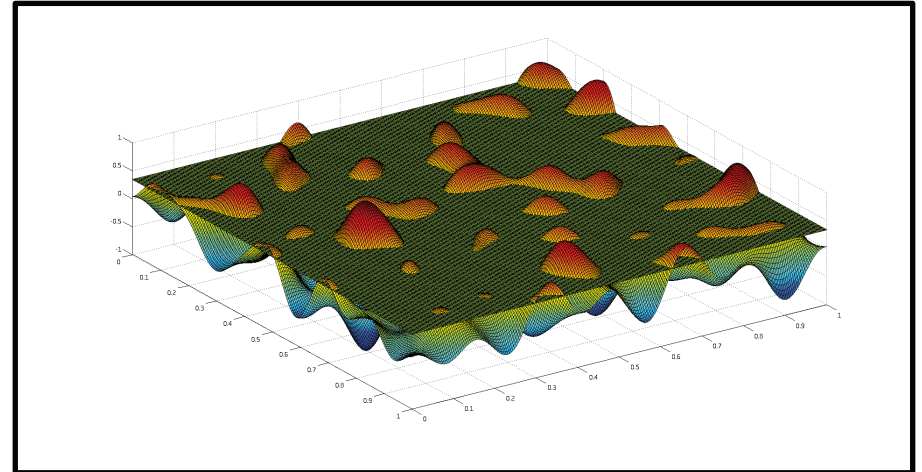
random Fourier series representation of surface topography

intersections of a plane with the surface define melt ponds

electronic transport in disordered media   *diffusion in turbulent plasmas*   *Isichenko, Rev. Mod. Phys., 1992*

Saddle Points, Morse Theory and the Fractal Geometry of Melt Ponds

Ryleigh Moore, Jacob Jones, Dane Gollero, Court Strong, Ken Golden 2021

snow
topography
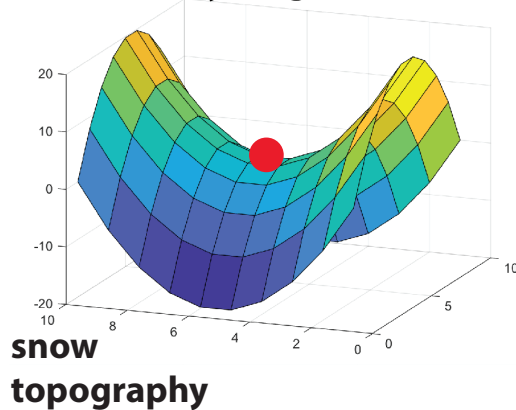
As ponds coalesce at saddle points, fractal dimension proxy isoperimetric quotient $P^2/4\pi A$ jumps, driving the transition.

Ryleigh Moore
Department of Mathematics
University of Utah

**Multidisciplinary drifting Observatory
for the Study of Arctic Climate (MOSAiC)**

MOSAiC School aboard the icebreaker *RV Akademik Federov*

20 grad students from around the world
(3 from U.S., 1 mathematician)

Ising Model for a Ferromagnet

M

T_c

T

**Curie point
critical temperature**
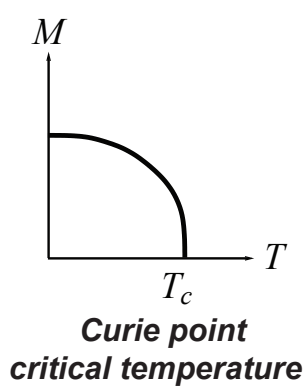
$$s_i = \begin{cases} +1 & \text{spin up} \\ -1 & \text{spin down} \end{cases}$$

blue

white

**applied
magnetic
field**

H

$$\mathcal{H} = -H \sum_i s_i - J \sum_{<i,j>} s_i s_j$$
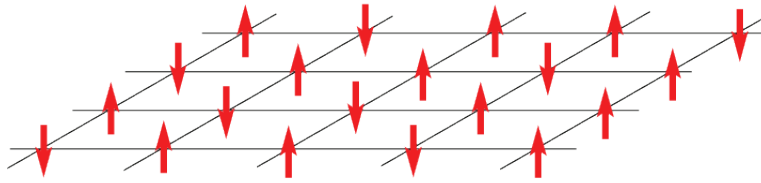
nearest neighbor Ising Hamiltonian

*islands of
like spins*

$$M(T, H) = \lim_{N \to \infty} \frac{1}{N} \left\langle \sum_j s_j \right\rangle$$

effective magnetization
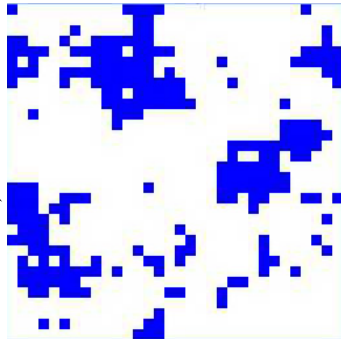
energy is lowered when nearby spins align
with each other, forming **magnetic domains**
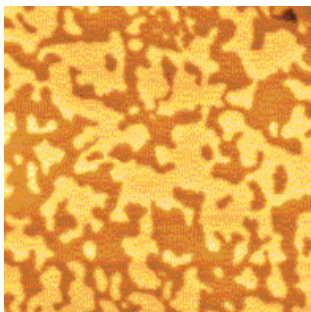
**magnetic domains
in cobalt**
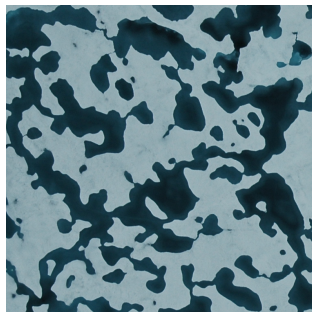
melt ponds (Perovich)
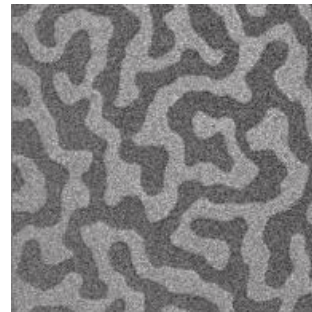
**magnetic domains
in cobalt-iron-boron**
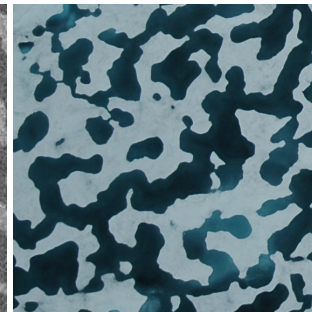
melt ponds (Perovich)

Ising model for ferromagnets ⟶ Ising model for melt ponds

$$\mathcal{H} = -\sum_{i}^{N} H_i \, s_i - J \sum_{<i,j>}^{N} s_i s_j \qquad s_i = \begin{cases} \uparrow & +1 \quad \text{water} \quad \text{(spin up)} \\ \downarrow & -1 \quad \text{ice} \quad\;\; \text{(spin down)} \end{cases}$$

random magnetic field represents snow topography

magnetization M **pond area fraction** ~ *albedo* $F = \dfrac{(M+1)}{2}$

only nearest neighbor patches interact

Starting with random initial configurations, as Hamiltonian energy is minimized by Glauber spin flip dynamics, system "flows" toward metastable equilibria.

Order from Disorder

pond size distribution exponent

observed   -1.5

(Perovich, *et al.* 2002)

model   -1.58

Ising model

melt pond photo (Perovich)

Scientific American EOS, PhysicsWorld, ...

ONLY MEASURED INPUT = LENGTH SCALE (GRID SIZE) from snow topography data

Melt ponds control transmittance of solar energy through sea ice, impacting upper ocean ecology.

WINDOWS

Perovich
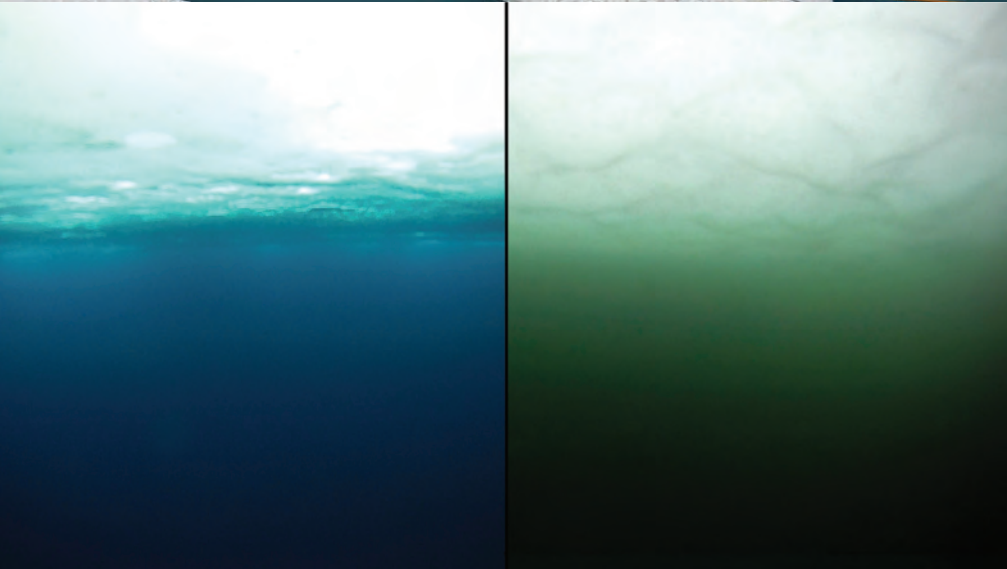
no bloom   bloom

massive under-ice algal bloom

Arrigo et al., *Science* 2012

Have we crossed into a new ecological regime?

The frequency and extent of sub-ice phytoplankton blooms in the Arctic Ocean

Horvat, Rees Jones, Iams, Schroeder, Flocco, Feltham, *Science Advances* 2017

The effect of melt pond geometry on the distribution of solar energy under first year sea ice

Horvat, Flocco, Rees Jones, Roach, Golden
Geophys. Res. Lett. 2019

(2015 AMS MRC)

macroscale

polar bear GPS

Ice floe diffusion in winds and currents

on short time scales floes
exhibit Brownian-like behavior

buoy data
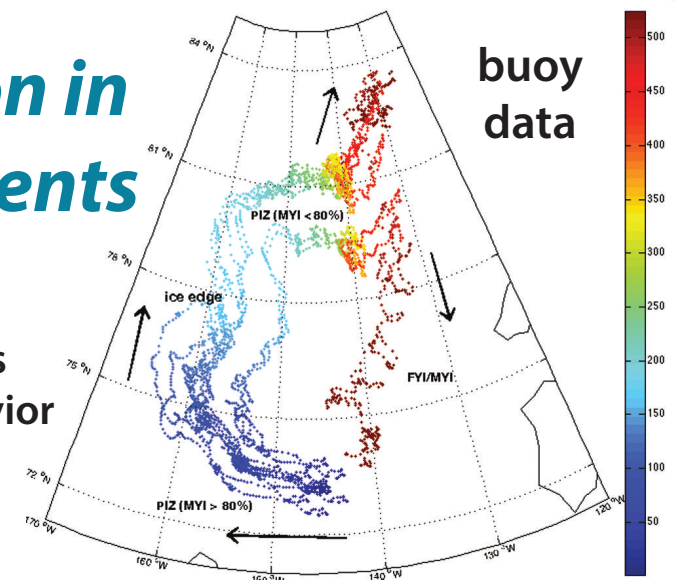
- Effective behavior is purely diffusive, sub-diffusive or super-diffusive depending on ice pack and advective conditions - **Hurst exponent.**

On sea-ice dynamical regimes in the Arctic Ocean

Jennifer Lukovich, Jennifer Hutchings, David Barber, *Ann. Glac.* 2015

Anomalous diffusion and sea ice dynamics

Huy Dinh, Ben Murphy, Elena Cherkaev, Ken Golden 2021

**floe-scale model - crowding
jamming, advective forcing**
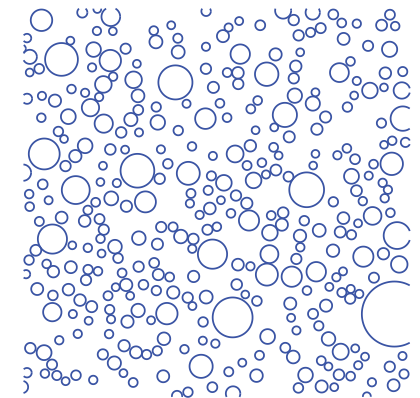
sea ice concentration = 0.3

Home ranges in moving habitats: polar bears and sea ice

Marie Auger-Méthé, Mark Lewis, Andrew Derocher, *Ecography*, 2016
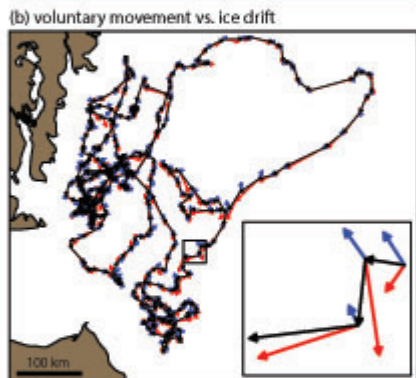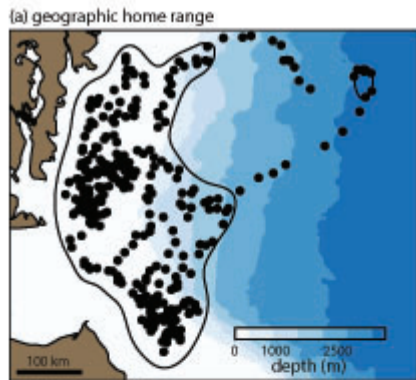
Filling the polar data gap with partial differential equations

hole in satellite coverage of sea ice concentration field

previously assumed ice covered

Gap radius: 611 km
06 January 1985
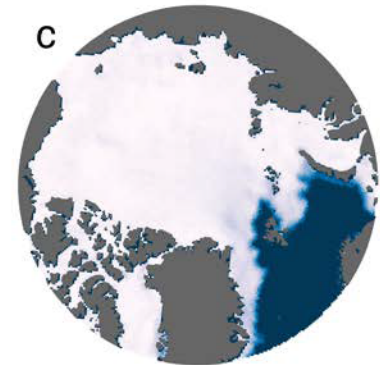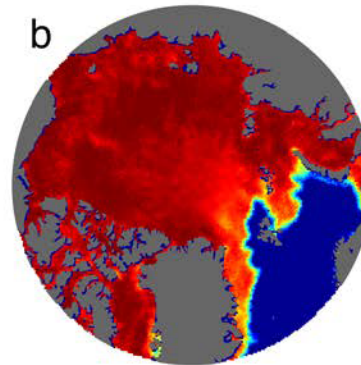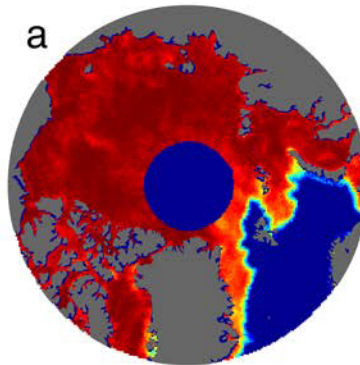
Gap radius: 311 km
30 August 2007
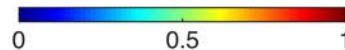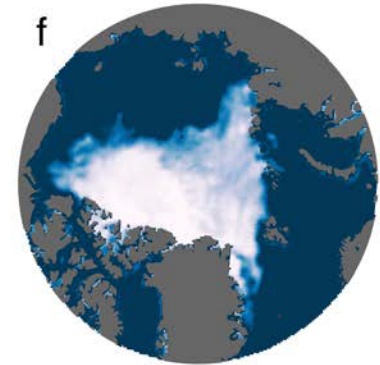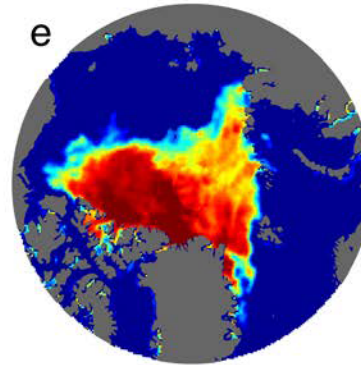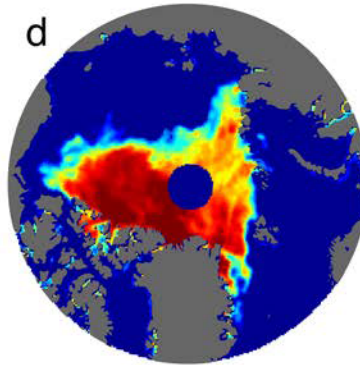
$$\Delta\psi=0$$

fill = harmonic function with learned stochastic term

Strong and Golden, *Remote Sensing* 2016
Strong and Golden, *SIAM News* 2017

NOAA/NSIDC Sea Ice Concentration CDR product update will use our PDE method.

Conclusions

1. Sea ice is a fascinating multiscale composite with structure similar to many other natural and man-made materials.

2. Mathematical methods developed for sea ice advance the theory of composites and other areas of science and engineering.

3. Homogenization and statistical physics help *link scales in sea ice and composites*; provide rigorous methods for finding effective behavior; advance sea ice representations in climate models.

4. Fluid flow through sea ice mediates melt pond evolution and many processes important to climate change and polar ecosystems.

5. Field experiments are essential to developing relevant mathematics.

6. Our research is helping to improve projections of climate change, the fate of Earth's sea ice packs, and the ecosystems they support.

University of Utah Sea Ice Modeling Group (2017-2021)

Senior Personnel: Ken Golden, Distinguished Professor of Mathematics
Elena Cherkaev, Professor of Mathematics
Court Strong, Associate Professor of Atmospheric Sciences
Ben Murphy, Adjunct Assistant Professor of Mathematics

Postdoctoral Researchers: Noa Kraitzman (now at ANU), Jody Reimer

Graduate Students: Kyle Steffen (now at UT Austin with Clint Dawson)
Christian Sampson (now at UNC Chapel Hill with Chris Jones)
Huy Dinh (now a sea ice MURI Postdoc at NYU/Courant)
Rebecca Hardenbrook
David Morison (Physics Department)
Ryleigh Moore
Delaney Mosier
Daniel Hallman

Undergraduate Students: Kenzie McLean, Jacqueline Cinella Rich,
Dane Gollero, Samir Suthar, Anna Hyde,
Kitsel Lusted, Ruby Bowers, Kimball Johnston,
Jerry Zhang, Nash Ward, David Gluckman

High School Students: Jeremiah Chapman, Titus Quah, Dylan Webb

---

Sea Ice Ecology Group   Postdoc Jody Reimer, Grad Student Julie Sherman,
Undergraduates Kayla Stewart, Nicole Forrester

Notices

of the American Mathematical Society

AMS
AMERICAN MATHEMATICAL SOCIETY
Advancing research. Creating connections.

THANK YOU

Office of Naval Research

Applied and Computational Analysis Program

Arctic and Global Prediction Program

National Science Foundation

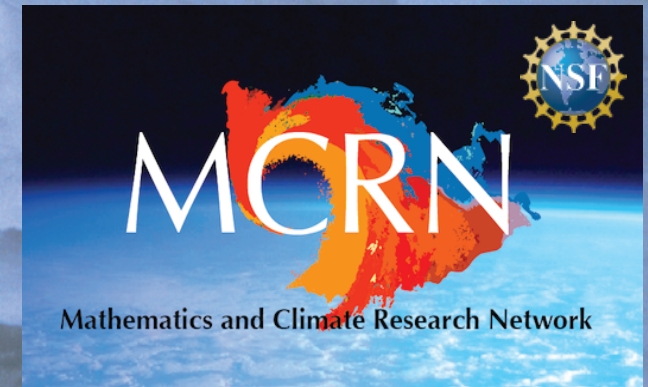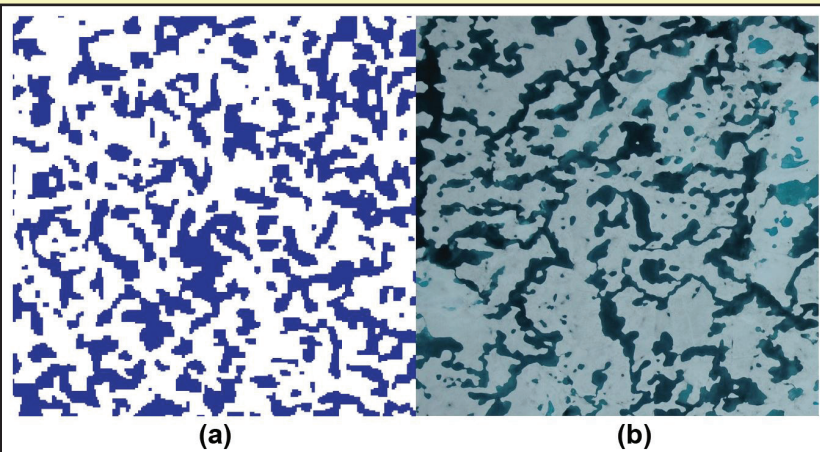Division of Mathematical Sciences

Division of Polar Programs

Buchanan Bay, Antarctica   Mertz Glacier Polynya Experiment   July 1999

siam news

Figure 3. *Comparison of real Arctic melt ponds with metastable equilibria in our melt pond Ising model.* **3a.** *Ising model simulation.* **3b.** *Real melt pond photo. Figure 3a courtesy of Yiping Ma, 3b courtesy of Donald Perovich.*

Vast labyrinthine ponds on the surface of melting Arctic sea ice are key players in the polar climate system and upper ocean ecology. Researchers have adapted the Ising model, which was originally developed to understand magnetic materials, to study the geometry of meltwater's distribution over the sea ice surface. In an article on page 5, Kenneth Golden, Yiping Ma, Courtenay Strong, and Ivan Sudakov explore model predictions.

Controlling Invasive Populations in Rivers

By Yu Jin and Suzanne Lenhart

Flow regimes can change significantly over time and space and strongly impact all levels of river biodiversity, from the individual to the ecosystem. Invasive species in rivers—such as bighead and silver carp, as well as quagga and zebra mussels—continue to cause damage. Management of these species may include targeted adjustment of flow rates in rivers, based on recent research that examines the effects of river morphology and water flow on rivers' ecological statuses. While many previous methodologies rely on habitat suitability models or oversimplification of the hydrodynamics, few studies have focused on the integration of ecological dynamics into water flow assessments.

Earlier work yielded a hybrid modeling approach that directly links river hydrology with stream population models [3]. The hybrid model's hydrodynamic component is based on the water depth in a gradually varying river structure. The model derives the steady advective flow from this structure and relates it to flow features like water discharge, depth, velocity, cross-sectional area, bottom roughness, bottom slope, and gravitational acceleration. This approach facilitates both theoretical understanding and the generation of quantitative predictions, thus providing a way for scientists to analyze the effects of river fluctuations on population processes.

When a population spreads longitudinally in a one-dimensional (1D) river with spatial heterogeneities in habitat and temporal fluctuations in discharge, the resulting hydrodynamic population model is

$$N_t = -A_t(x,t)\frac{N}{A(x,t)} +$$

$$\frac{1}{A(x,t)}\Big(D(x,t)A(x,t)N_x\Big)_x -$$

$$\frac{Q(t)}{A(x,t)}N_x + rN\left(1-\frac{N}{K}\right)$$

$$N(0,t)=0 \qquad \text{on } (0,T), x=0,$$
$$N_x(L,t)=0 \qquad \text{on } (0,T), x=L,$$
$$N(x,0)=N_0(x) \qquad \text{on } (0,L), t=0$$

$$(1)$$

Modeling Resource Demands and Constraints for COVID-19 Intervention Strategies

By Erin C.S. Acquesta, Walt Beyeler, Pat Finley, Katherine Klise, Monear Makvandi, and Emma Stanislawski

As the world desperately attempts to control the spread of COVID-19, the need for a model that accounts for realistic trade-offs between time, resources, and corresponding epidemiological implications is apparent. Some early mathematical models of the outbreak compared trade-offs for non-pharmaceutical interventions [3], while others derived the necessary level of test coverage for case-based interventions [4] and demonstrated the value of prioritized testing for close contacts [7].

Isolated analyses provide valuable insights, but real-world intervention strategies are interconnected. Contact tracing is the lynchpin of infection control [6] and forms the basis of prioritized testing. Therefore, quantifying the effectiveness of contact tracing is crucial to understanding the real-life implications of disease control strategies.

Contact Tracing Demands

Contact tracers are skilled, culturally competent interviewers who apply their knowledge of disease and risk factors when notifying people who have come into contact with COVID-19-infected individuals. They also continue to monitor the situation after case investigations [1].

Case investigation consists of four steps:
1. Identify and notify cases
2. Interview cases
3. Locate and notify contacts
4. Monitor contacts.

Most health departments are implementing case investigation, contact identification, and quarantine to disrupt COVID-19 transmission. The timeliness of contact tracing is constrained by the length of the infectious period, the turn-around time for testing and result reporting, and the ability to successfully reach and interview patients and their contacts. The European Centre for Disease Prevention and Control approximates that contact tracers spend one to two hours conducting an interview [2]. Estimates regarding the timelines of other steps are limited to subject matter expert elicitation and can vary based on cases' access to phone service or willingness to participate in interviews.

Bounded Exponential

The fundamental structure of our model follows traditional susceptible-exposed-infected-recovered (SEIR) compartmental modeling [5]. We add an asymptomatic population A, a hospitalized population H, and disease-related deaths D, as well as corresponding quarantine states. We define the states $\{S_i, E_i, A_i, I_i, H, R, D\}_{i=0,1}$ for our compartments, such that $i=0$ and $i=1$ correspond to unquarantined and quarantined respectively. Rather than focus on the dynamics that are associated with the state transition diagram in Figure 1, we introduce a formulation for the real-time demands on contact tracers' time as a function of infection prevalence, while also respecting constraints on resources.

When the work that is required to investigate new cases and monitor existing contacts exceeds available resources, a backlog develops. To simulate this backlog, we introduce a new compartment C for tracking the dynamic states of cases:

$$\frac{dC}{dt}=[flow_{in}]-[flow_{out}].$$

Flow into the backlog compartment, represented by $[flow_{in}]$, reflects case identification that is associated with the following transitions in the model:

– The rate of random testing: $q_{rA}(t)A_0(t)\rightarrow A_1(t)$ and $q_{rI}(t)I_0(t)\rightarrow I_1(t)$
– Testing triggered by contact tracing: $q_{tA}(t)A_0(t)\rightarrow A_1(t), \quad q_{tI}(t)I_0(t)\rightarrow I_1(t),$ and $q_{tE}(t)E_1(t)\rightarrow\{A_1(t),I_1(t)\}$
– The population that was missed by the non-pharmaceutical interventions that require hospitalization: $\tau_{IH}(t)I_0(t)\rightarrow H(t).$

Here, $q_{r*}(t)$ defines the time-dependent rate of random testing, $q_{t*}(t)$ signifies the time-dependent rate of testing that is triggered by contact tracing, and τ_{IH} is the inverse of the expected amount of time for which an infected individual is symptomatic before hospitalization. These terms collectively provide the simulated number of newly-identified positive COVID-19 cases. However, we also need the average number of contacts per case. We thus define function $\mathcal{K}(\kappa,T_S,\phi_\kappa)$ that depends on the average number of contacts a day (κ), the average number of days for which an individual is infectious before going into isolation (T_S), and the likelihood that the individual
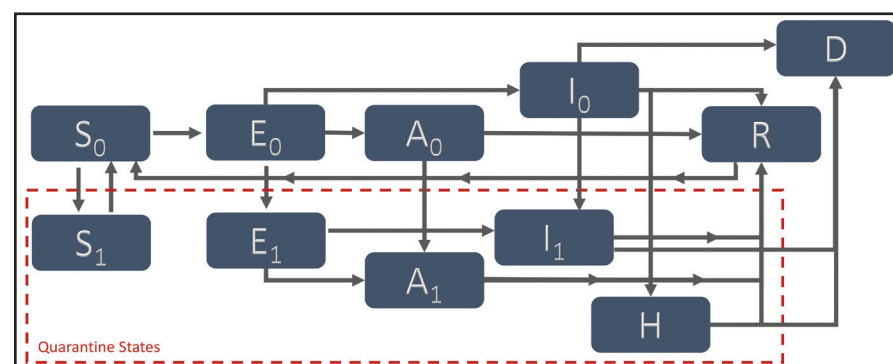
Figure 1. *Disease state diagram for the compartmental infectious disease model. Figure courtesy of the authors.*

Modeling Sea Ice

Kenneth M. Golden, *Luke G. Bennetts,*
Elena Cherkaev, *Ian Eisenman, Daniel Feltham,*
Christopher Horvat, Elizabeth Hunke,
Christopher Jones, Donald K. Perovich,
Pedro Ponte-Castañeda, *Courtenay Strong*,
Deborah Sulsky, and Andrew J. Wells

Kenneth M. Golden is a Distinguished Professor of Mathematics at the University of Utah. His email address is golden@math.utah.edu.

Luke G. Bennetts is an associate professor of applied mathematics at the University of Adelaide. His email address is luke.bennetts@adelaide.edu.au.

Elena Cherkaev is a professor of mathematics at the University of Utah. Her email address is elena@math.utah.edu.

Ian Eisenman is an associate professor of climate, atmospheric science, and physical oceanography at the Scripps Institution of Oceanography at the University of California San Diego. His email address is eisenman@ucsd.edu.

Daniel Feltham is a professor of climate physics at the University of Reading. His email address is d.l.feltham@reading.ac.uk.

Christopher Horvat is a NOAA Climate and Global Change Postdoctoral Fellow at the Institute at Brown for Environment and Society at Brown University. His email address is christopher_horvat@brown.edu.

Elizabeth Hunke is a deputy group leader, T-3 fluid dynamics and solid mechanics group at the Los Alamos National Laboratory. Her email address is eclare@lanl.gov.

Christopher Jones is a Bill Guthridge Distinguished Professor of Mathematics at the University of North Carolina, Chapel Hill. His email address is ckrtj@unc.edu.

Donald K. Perovich is a professor of engineering at the Thayer School of Engineering at Dartmouth College. His email address is donald.k.perovich@dartmouth.edu.

Pedro Ponte-Castañeda is a Raymond S. Markowitz Faculty Fellow and professor of mechanical engineering and applied mechanics and of mathematics at the University of Pennsylvania. His email address is ponte@seas.upenn.edu.

Courtenay Strong is an associate professor of atmospheric sciences at the University of Utah. His email address is court.strong@utah.edu.

Deborah Sulsky is a professor of mathematics and statistics and of mechanical engineering at the University of New Mexico. Her email address is sulsky@math.unm.edu.

Andrew J. Wells is an associate professor of physical climate science at the University of Oxford. His email address is Andrew.Wells@physics.ox.ac.uk.

Marginal Ice Zone
MIZ

- biologically active region
- intense ocean-sea ice-atmosphere interactions
- region of significant wave-ice interactions

transitional region between
dense interior pack ($c > 80\%$)
sparse outer fringes ($c < 15\%$)
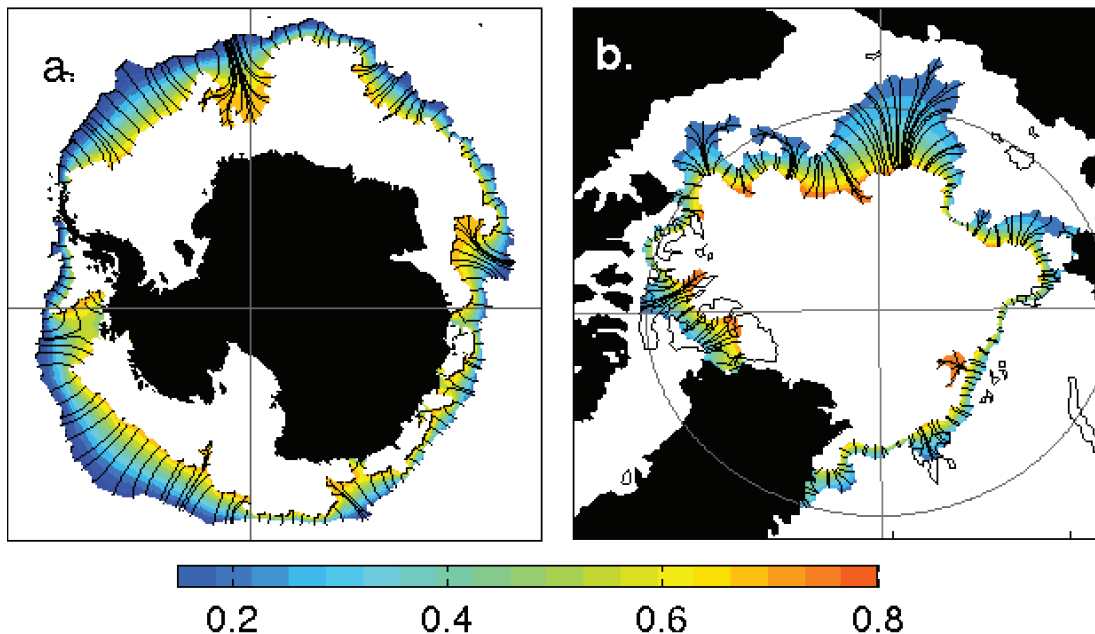
MIZ WIDTH
fundamental length scale of
ecological and climate dynamics

Strong, *Climate Dynamics* 2012
Strong and Rigor, *GRL* 2013

**How to objectively
measure the "width"
of this complex,
non-convex region?**

Objective method for measuring MIZ width motivated by medical imaging and diagnostics

Strong, *Climate Dynamics* 2012
Strong and Rigor, *GRL* 2013

39% widening
1979 - 2012

"average" lengths of streamlines

streamlines of a solution to Laplace's equation
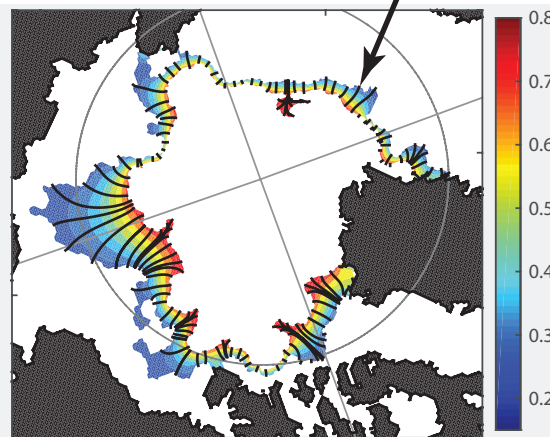
Arctic Marginal Ice Zone
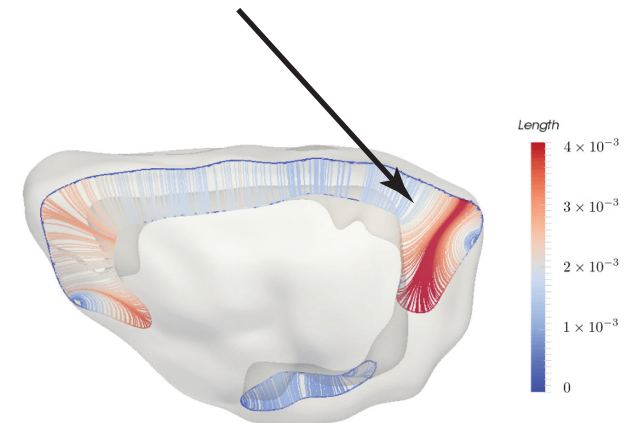
crossection of the cerebral cortex of a rodent brain

analysis of different MIZ WIDTH definitions

Strong, Foster, Cherkaev, Eisenman, Golden
J. Atmos. Oceanic Tech. 2017

Fire endangers Hobart's ice ship

By DAVID CARRIGG

AN engine-room fire has left the Hobart-based Antarctic research ship Aurora Australis without power in dangerous sea ice off the Antarctic coast.

None of the 79 people on board was injured in the blaze, which broke out early yesterday morning while the ship was in deep water 185km off the coast.

The extent of the damage is not known.

Australian Antarctic Division director Rex Moncur said the fire was extinguished by flooding the engine room with an inert gas.

The gas had to be cleared before crew wearing breathing apparatus could enter and assess the situation.

He said it could be some time before the extent of damage was known.

The 25 crew and 54 expeditioners, mostly from Hobart, would wear thermal clothing and stay below decks to keep warm.

"There is always a risk of becoming ice-bound in these waters at this time of the year but at this stage we don't expect to launch a rescue mission from Hobart," Mr Moncur said.

The ship was in regular radio contact with the Antarctic Division's Hobart office.

He expected the expeditioners and crew to abandon the pioneering winter voyage and return the ship to Hobart for repairs in about a week.

The Antarctic Division, which hires the ship from P&O Australia, would not be hiring another vessel for the expedition.

"It's a pretty specialist vessel so you couldn't get the sort of research capability that this ship has got readily available," Mr Moncur said.

"We hope the next voyage can still proceed on schedule, which is early September."

The Aurora Australis is owned by P&O Australia and charted by the Antarctic Division for about $11 million a year.

P&O Australia managing director Richard Hein said yesterday the company was assessing the situation and a number of rescue options were being considered.

It was too early to say whether P&O would be liable for the cost of the aborted mission.

The vessel left Hobart last Wednesday for a seven-week voyage mainly to study a polynya, an area where savage winds break up the sea ice and cause heavy, salt-laden water to sink to the bottom.

The ship was nearing the polynya when the fire broke out.
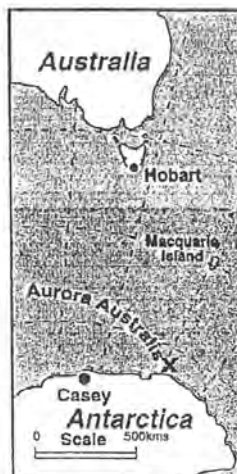
Oceanographers believe a closer study of the phenomenon will lead to a better understanding of climate change.

CSIRO Marine Research oceanographer Steve Rintoul said the dense bottom water, created only in a few places in Antarctica and to a lesser extent in the North Atlantic, was critical to the chemistry and biology of the world's oceans.

A file photo of the Aurora Australis in Antarctica.

Fire strands Antarctic ship in sea ice

AN engine room fire has disabled the icebreaker Aurora Australis in sea ice, deep in Antarctic waters.

There were no injuries and the ship was not in danger after Tuesday night's fire.

Australian Antarctic Division director Mr Rex Moncur said. But Mr Moncur said he expected it would have to abandon its pioneering mid-winter voyage to the edge of the Antarctic continent and return to Hobart for repairs.

The cause of the fire was not known but the engines have been turned off, with the ship 100 nautical miles from the Antarctic coast.

Antarctic voyage stopped by fire

HOBART: An engine room fire has disabled the Australian icebreaker Aurora Australis in sea ice, deep in Antarctic waters.

Australian Antarctic Division director Rex Moncur said there were no injuries and the ship was not in danger after Tuesday night's fire.

But Mr Moncur said he expected Aurora Australis would have to abandon its pioneering mid-winter voyage to the edge of the Antarctic continent to return to Hobart for repairs.

The fire had been extinguished and the engines were turned off, leaving the ship in sea ice about 100 nautical miles from the Antarctic coast, he said. The weather was good.

Crew had to wear breathing apparatus to enter the engine room and it was likely to be 24 hours before the damage could be fully assessed.

The Aurora, with 54 expeditioners and 25 crew, left Hobart last Wednesday for a seven-week voyage which was to have focused on a polynya, an area where savage winds break up the sea ice and cause heavy, salt-laden water to sink to the bottom.

Mr Moncur said, the cause of the fire was not yet known.

Sydney Morning Herald
23 July, 1998

ICEBREAKER BURNS

A pioneering $2 million Australian scientific voyage to the mid-winter Antarctic pack ice is expected to be scrapped following an engine-room fire on the Aurora Australis yesterday. The 54 people on board were forced on deck in the ...

2:45 am July 22, 1998

``Please don't be alarmed but we have an uncontrolled fire in the engine room ...."

about 10 minutes later ...

``Please don't be alarmed but we're lowering the lifeboats ...."